



1950-2100 climate trends in avalanche activity in Haute-Maurienne, French Alps

François Doussot¹, Léo Viallon-Galinier¹, Nicolas Eckert², and Pascal Hagenmuller¹

¹Météo-France, CNRS, Univ. Grenoble Alpes, Univ. Toulouse, CNRM, Centre d'Études de la Neige, 38000 Grenoble, France

²Univ. Grenoble Alpes, INRAE, CNRS, IRD, Grenoble INP, IGE, Grenoble, France

Correspondence: François Doussot (francois.doussot@meteo.fr)

Abstract. Avalanche activity in alpine regions is sensitive to climate change. However, without consistent historical data, it is challenging to estimate past trends in avalanche activity and assess future avalanche scenarios from climate projections. To tackle this challenge, we use avalanche observations and simulated snowpack conditions to train a machine learning gradient-boosting regression model, which predicts the number of avalanches per day. We focus on a small alpine domain with high-quality data: the Haute-Maurienne valley in the French Alps, where avalanche paths span elevations from approximately 1800 to 2700 m a.s.l. First, we demonstrate that accounting for the uncertainties in avalanche occurrence dates and using only the most recent period (2006–2023) with homogeneous observations during the training step is essential for achieving consistent results. We then use this machine learning model to reconstruct the past avalanche activity (1958–2023) from reanalysed meteorological and snow data, and to project future avalanche activity (1950–2100) from a downscaled ensemble of snow-climate simulations. We evaluate climatic trends in avalanche activity using three indicators: the number of avalanches per winter season, the number of avalanches per month, and the annual maximum number of avalanches in one week, which quantifies the largest avalanche cycles. Based on reanalysed snow-climate simulations, the model estimates that avalanche activity decreased in the past: the mean number of avalanches per year declined by approximately 9% per decade between 1958 and 2023, with a stronger decrease in spring avalanche activity, and the 30-year return level associated with large avalanche cycles decreased at a slower rate of around 4% per decade. In the future, avalanche activity is also expected to decrease. For the emission scenarios RCP4.5 and RCP8.5, the annual number of avalanches is expected to decrease by around 5% and 9% per decade, respectively, mainly due to a reduction in spring avalanche activity. Large avalanche cycles, quantified by the 30-year return level, are also expected to decrease in intensity but at slower rates: around 2% per decade for RCP4.5 and 5% per decade for RCP8.5. This study quantifies the impact of climate change on avalanche activity in an exemplary alpine valley. It demonstrates that combining statistical learning with climate simulations can help produce reference scenarios for mitigation strategies in high mountain environments.

1 Introduction

Snow avalanches are rapid mass movements of snow down a steep slope (Schweizer et al., 2003). They represent a significant natural hazard in snow-covered mountainous regions, threatening human lives, settlements, and infrastructure. Studying



25 avalanche risk is essential in populated areas of mountainous regions, such as the European Alps, due to the economic and
human stakes involved (Fuchs et al., 2007; Cappabianca et al., 2008; Eckert et al., 2012; Techel et al., 2016). In these areas,
mitigation strategies are mandatory and mainly rely on heavy protective structures or restrictive land-use policies, which are
designed to remain effective over several decades (Höller, 2007). Therefore, implementing effective risk mitigation strategies
requires anticipating potential non-stationarity in risk components, among which is the possible impact of climate change on
30 avalanches (Fuchs et al., 2013; Eckert and Giacoma, 2023).

The frequency, magnitude, and spatial distribution of avalanches are closely related to snowpack conditions (Schweizer et al., 2003), i.e. the quantity and quality of the snow on the ground. Their evolution with climate change is the primary driver of climatic trends in avalanche activity and is thus briefly described here for the European Alps (e.g. Dumont et al., 2025). Durand et al. (2009) reported a marked decline in snow depth in the French Alps between 1958 and 2005, with the most
35 significant reductions observed at the lowest elevations and at the end of the winter season. Matiu et al. (2021) quantified this shortening of the snow season by roughly one month since 1950, below 2000 m elevation in the European Alps. The reduction in snow on the ground is primarily attributed to rising air temperatures, which cause precipitation to change from a solid to a liquid state (Serquet et al., 2011). Meanwhile, mean precipitation amounts are almost constant (Bozzoli et al., 2024; Masson and Frei, 2015). Therefore, the impact of climate change is strongly dependent on elevation: at relatively high altitude sites
40 such as Weissfluhjoch (located at 2536 m in the Swiss Alps), mean winter snow depth has remained nearly constant between 1960 and 2023 because the warming in winter has not been sufficient to shift precipitation from snow to rain (Dumont et al., 2025). Future trends were computed from climate simulations downscaled on the complex topography of alpine regions (e.g., Marty et al., 2017; Verfaillie et al., 2018; Kotlarski et al., 2023). Marty et al. (2017) demonstrated that the resulting snow cover changes may be roughly equivalent to an elevation shift of 500 to 1000 m by the end of the century depending on the
45 emission scenarios. Verfaillie et al. (2018) showed that the impact of emission scenarios becomes significant for the second half of the 21st century. While the mean winter snow depth is expected to decrease, climate change may also impact other snowpack properties. The snowpack will be wetter, and rain-on-snow events are expected to increase (Beniston and Stoffel, 2016). Extreme snowfall events will also be impacted: by the end of the century, they are expected to decrease in the Pyrenees (Bonsoms et al., 2025), as in the French Alps under 2700 m, but the 100-year return level of daily snowfall above 2700 m -
50 3000 m is expected to stay constant or to increase slightly (Le Roux et al., 2023). The decrease in mean winter snow depth might also be accompanied by shifts in the physical properties of the snowpack, as the snow metamorphism is dependent on the temperature gradient (Schneebeli and Sokratov, 2004). Because snow microstructure has a primary influence on snowpack stability (Schweizer et al., 2003), the combined effects of changing snow depth, snow layer properties, and resulting snow microstructure make the overall impact on snowpack stability difficult to assess.

55 One direct way to estimate past climate trends in avalanche activity is to assess it in a consistent, representative spatial domain using a fixed sampling strategy over several decades. Whereas satellite monitoring is a promising tool (Karas et al., 2022) to acquire data in a systematic way, this new technology lacks temporal coverage to capture anthropogenic climate trends above the decadal internal climate variability (Hafner et al., 2021). Given that systematic measurements are rare, multi-source historical archives (e.g., administrative documents, newspapers) (Giacoma et al., 2017, 2022), or proxy records, such as tree



60 rings (Corona et al., 2012), seismic signals (Heck et al., 2018) or geomorphic markers (Johnson and Smith, 2010) are often used (Eckert et al., 2024). For instance, Giacoma et al. (2021) used historical records and statistical techniques to examine the impact of long-term past climate change on avalanche activity in the low-elevation Vosges Mountains, France. The study mainly revealed a transition from the late Little Ice Age to the early twentieth century, with a drastic reduction in the annual number of avalanches. Peitzsch et al. (2021) used tree rings to quantify a decline of about 14% in avalanche activity in the
65 Rocky Mountains between 1950 and 2017. In a higher mountain environment, Ballesteros-Cánovas et al. (2018) demonstrated an increase in avalanche activity in the western Indian Himalayas, using dendrochronology in avalanche paths located between 2,600 and 4,200 m elevation, but the study was limited to a few slopes. In the French Alps, the *Enquête Permanente sur les Avalanches* (EPA) reports avalanche activity observed in numerous and specified avalanche paths since the early twentieth century (Bourova et al., 2016). It is thus likely to vary over time with human factors and formal task instructions, creating
70 biases in trends and thereby precluding inference of climatic control. Although the influence of an individual observer may be negligible at the scale of entire mountain ranges, where large-scale trends can still emerge despite local observational artefacts (Eckert et al., 2010d), this influence becomes critical in contexts where the observation record relies on only a limited number of observers. The temporal resolution of such observations is high - a few days - compared to indirect observations, but still too coarse to capture the correlation to snow conditions evolving within hours. Based on this EPA dataset for the period 1950-2009,
75 Eckert et al. (2013) reported a peak in avalanche activity in the 1980s in the French Alps, followed by a 19% decrease in the mean number of avalanches per winter through 2009. Due to unknown sampling variations over time, it is, however, almost impossible to evaluate to which extent this overall trend is altered over smaller domains.

80 Capturing future trends from direct or indirect avalanche observations is by definition impossible. Projecting avalanche activity necessarily requires linking climate simulations forced by emission scenarios to snow conditions and finally to avalanche activity. The main idea is to build a relationship between snow conditions and avalanche activity using either physical knowledge of the involved processes or machine learning techniques on a reference period, where the targeted avalanche activity and predictive snow conditions are known with sufficient accuracy. This impact model can then be applied to snow simulations forced by downscaled climate simulations. This strategy also works on the past, with a forcing based on reanalysed meteorological data. We employ this strategy in the paper and briefly review here the studies which used similar methods to capture
85 climate-driven trends in avalanche activity. Reuter et al. (2025) developed a physically-based model to relate simulated snow conditions to avalanche problems. Applied to the S2M reanalysis (Vernay et al., 2022) on the French Alps over 1958-2020, they showed a decreasing frequency of persistent weak layer problems, an increasing frequency of new snow problems and that the onset of wet-snow activity now occurs about three weeks earlier than in 1958. This study provides clues about the evolution of the main drivers of avalanche activity but lacks quantification of the severity of the detected avalanche problems.
90 Castebrunet et al. (2014) pioneered the projection of future avalanche activity. They used a statistical regression model fitted on observed avalanches and simulated snow conditions at the French Alps scale. Based on the global trajectories of the CMIP4 framework (Nakicenović and Swart, 2000), they showed a general decrease in avalanche activity for the whole domain and observed inconsistent evolutions at high altitude. Ortner et al. (2025) investigated future changes in avalanche risks and the associated monetary loss in the Central Swiss Alps. They built a hazard map based on the avalanche flow RAMMS forced



95 by the projected three-day snow depth accumulation and temperature, which is then combined with the vulnerability of the exposed infrastructures. The results show a marked decline in the average annual impact of avalanches by the end of the century. However, it should be noted that this integrated approach, from climate simulations to monetary costs, remains relatively simple at the avalanche formation step. Indeed, the study assumes that any three-day snowfall can, without distinction, trigger an avalanche and that factors known to contribute to avalanche formation, such as wind, pre-existing snowpack, and snow
100 wetting, are omitted. Mayer et al. (2024) used a snow cover model driven by downscaled climate simulations to compute future alterations in dry- and wet-snow avalanche occurrences throughout the 21st century across seven sites in the Swiss Alps. Their machine learning model classifies each day as either a non-avalanche day, a dry-snow avalanche day or a wet-snow avalanche day. The results show a decrease in the overall annual number of avalanche days until 2100, by 20-40% relative to the RCP8.5 scenario, and approximately 10% relative to the RCP4.5 scenario. To date, Mayer et al. (2024) has provided one of the most
105 comprehensive studies of projected changes in avalanche activity under a warming climate. However, the binary classification of avalanche and non-avalanche days does not provide information about the intensity of the avalanche cycle, which is of great importance for mitigation strategies.

110 In short, the big picture of changes in avalanche activity under a warming climate is already rather clear: fewer and fewer avalanches, on average, as temperature increases. This decreasing trend is exacerbated where the snowpack vanishes, i.e., at lower elevations or at the end of the snow season (Eckert et al., 2024). However, at higher elevations and for high-impact avalanche cycles, the picture is less clear and lacks support by quantitative findings. Long and consistent observational series are rare, and indirect sources such as historical archives or tree rings provide trends at annual/seasonal resolution only. Human-based inventories introduce observer biases and uncertainties that may blur true climatic signals. Model-based studies, whether physical, statistical, or machine learning, generally simplify key processes and often provide broad patterns without quantifying
115 the actual intensity of avalanche cycles. There are thus many gaps in the current understanding of the impact of climate change on avalanche activity.

120 In this study, we focus on a populated valley in the French Alps, the Haute-Maurienne, and quantify changes in avalanche activity between 1950 and 2100. This valley is a model territory at the European scale: frequent avalanches affect human activities, it is a relatively high elevation site, and avalanches have been systematically reported in recent decades. We characterize the changes in avalanche activity not only by the average number of avalanches per year but also by the seasonality of avalanche occurrence and the return period of intense avalanche cycles. To capture the link between snow conditions and avalanches, we train a machine learning model on a human-based avalanche inventory and reanalysed weather and snow simulations. The training step accounts for potential biases and uncertainties in the inventory, and the set of predictors is comprehensive enough to capture the complex and multivariate daily relationship between snow and avalanches. To reconstruct the past or project the
125 future of avalanche activity, we use the best meteorological dataset available to date for the considered spatio-temporal domain as input to our machine learning model.



2 Material and methods

2.1 Overall approach

We developed a machine learning model that predicts the daily number of avalanches per aspect sector from simulated weather and snowpack conditions, after training on a human-based avalanche inventory. Similar to Sielenou et al. (2021); Mayer et al. (2022); Viallon-Galinier et al. (2023); Hendrick et al. (2023), we relate daily meteorological and snow conditions to daily avalanche activity. We split the area under study into four aspect sectors: North, East, South, and West-oriented sectors, as snow-related variables depend heavily on incoming solar radiation.

In this section, we first present the target variable (i.e., the variable we want to predict): the daily number of avalanches in the Haute-Maurienne valley, as reported by the EPA inventory. Next, we describe the model input features (i.e., predictors of the target variable). These features are either derived from reanalysed weather and snow data or from snow-climate simulations. Then, we detail the machine learning model itself. In particular, we describe how we account for uncertainties and biases in the avalanche observations. Finally, we define three indicators derived from the daily prediction that we use to evaluate the model and quantify avalanche activity.

2.2 Target: daily number of avalanches per aspect sector

The *Enquête Permanente sur les Avalanches* (EPA) is a French survey that reports all avalanches that meet a specified threshold on designated avalanche paths (Bourova et al., 2016; Eckert et al., 2010a). Approximately 3900 avalanche paths are monitored in France, mainly by operators of the forestry service (Eckert et al., 2013). Each path has an associated flow threshold, and any avalanche that exceeds this threshold is expected to be included in the inventory. Each reported avalanche is at least described by the associated path and the time window during which it occurred. Each path is characterized by the average aspect and altitude of the typical release zone. One of the main advantages of this dataset is its presumed temporal homogeneity, as the flow thresholds have remained unchanged over the years. However, the EPA has been rigorously revised after the Montroc avalanche in 1999 and, in 2006, the observation protocol was revised, including the addition of new descriptors of the avalanches (Bourova et al., 2016). A second advantage of the EPA is that avalanches are reported almost daily. The occurrence of an avalanche is controlled by the snow conditions at the time it occurred, and is only very weakly controlled, for instance, by the snow conditions averaged over the winter season (Schweizer et al., 2003). To learn the relationship between snow conditions and avalanche occurrence, it is thus important to rely on data of high temporal resolution of the order one day. However, the EPA is not perfect in this aspect: for each avalanche event recorded, the observer identifies a time window defined by two days [d_1 , d_2] during which the avalanche probably occurred. This period may correspond either to the interval between two successive observations or to a narrower time frame based on the observer's evaluation of meteorological and snow conditions. The length of this interval is rarely one day but generally spans one to five days due to avalanche danger, visibility conditions, holidays, etc. Lastly, it should be noted that the EPA dataset does not inventory all avalanches but only those in pre-designated paths. This survey was primarily developed for risk management in areas near the valley floor, so avalanches in unpopulated areas or those threatening snow recreationists are far from all included.

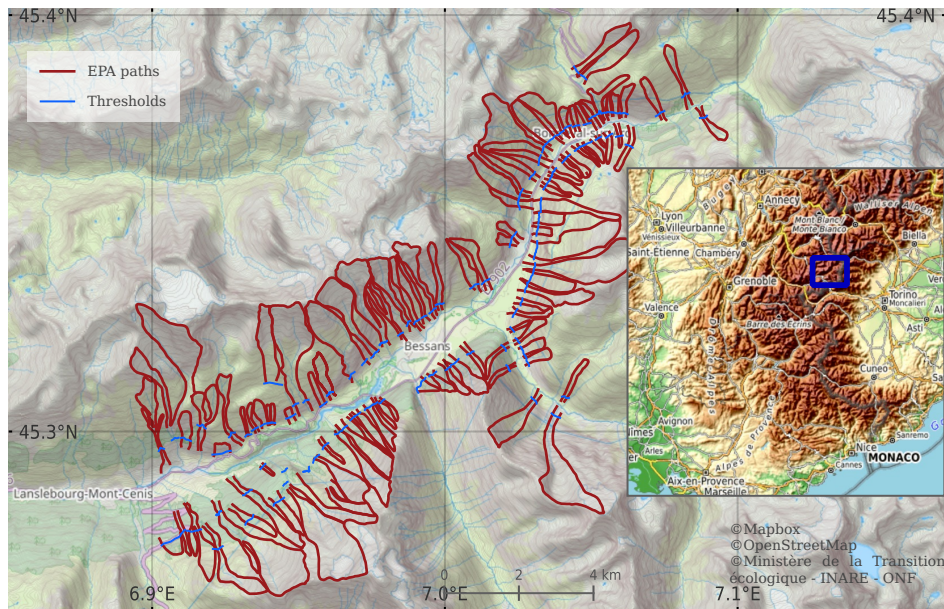


Figure 1. EPA paths in the selected area of the Haute-Maurienne valley.

160 This study focuses on the Haute-Maurienne valley, located in the French Alps. This valley has long been a critical area for
avalanche observation due to its geography, with relatively high mountains and steep avalanche paths (e.g. Kern et al., 2020;
Zgheib et al., 2020; Viallon-Galinier et al., 2023; Barkat et al., 2024). We focus on the upper valley, which is characterized
by more active avalanche paths. The study area comprises the three district municipalities of Bessans, Bonneval-sur-Arc and
Lanslevillard (Fig. 1). It is characterized by about a hundred monitored EPA avalanche paths and thousands of avalanches have
165 been recorded between 2006 and 2023. The typical flow threshold is at an elevation around 1800 m (slightly above the valley
bottom) while the avalanche paths extend to maximum elevations of up to 3300 m, with an average upper limit of about 2700
m. On this subset, the observations show almost no avalanches in the 1950s and a strong avalanche activity in the last decades
(Fig. 2), which is inconsistent with larger-scale trends (Eckert et al., 2013). This behavior may be specific to the considered
170 domain. The number of days of uncertainty associated with each avalanche release date is variable: the exact day a given
avalanche occurred is known only in about 18% of the cases and 96% of the avalanche occurrence days are known with less
than five days of uncertainty (Fig. 3).

175 In practice, we filtered the raw avalanche events recorded in the EPA to overcome its limitations. First, we excluded the data
prior to the last renovation of the observation protocol in 2006 to evaluate the machine learning model, considering only the
period spanning from winter 2006/2007 to winter 2022/2023. Second, we assumed that an event reported in the time window
[d_1, d_2] occurred between 18:00 UTC on day $d_1 - 1$ and d_2 at 18:00 UTC. We also chose to exclude events with more than five
days of uncertainty from this analysis, which correspond to 3.6% of the listed events. In other words, we arbitrarily assumed
that these very uncertain but sporadic events never happened. Third, we considered only the paths that have been monitored



during the entire period 2006-2023. This final filtered dataset consists of $n = 89$ EPA avalanche paths and $m = 2080$ recorded avalanches between 2006 and 2023.

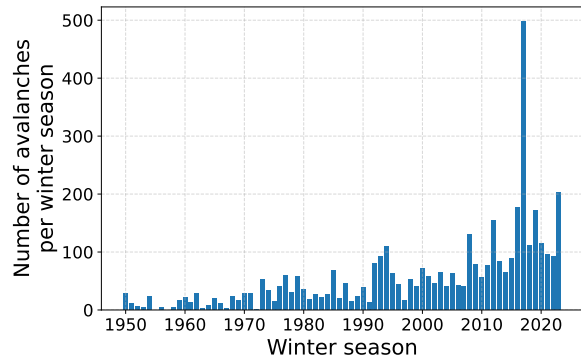


Figure 2. Raw number of avalanches reported in the EPA dataset from 1950 to 2023.

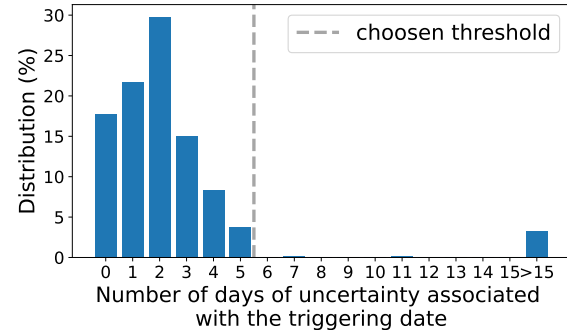


Figure 3. Distribution of the number of days of uncertainty concerning the triggering date from 2006 to 2023.

180 2.3 Features: weather and snowpack

The input features for the machine learning model are generated from a series of models. An atmospheric model provides input data to a snowpack model, which simulates the evolution of snowpack stratigraphy. From this, various predictors related to avalanche formation are calculated.

2.3.1 Weather forcings

185 We used two types of weather forcings: reanalysed meteorological data and climate simulations. These forcings define the spatial resolution of the model chain. It is produced over elementary areas designed to represent the main drivers of spatial variability in mountains: the so-called “massifs” (here Haute-Maurienne), segmented into different elevation bands (here 1800, 2100, 2400 and 2700 m), aspects (here N, E, S, W) and slope angles (here, 40 degrees). The weather forcings are generated at hourly resolution.

190 To study past weather and snow conditions, we used the SAFRAN meteorological reanalysis, which provides meteorological data for the period 1958-2023 (Vernay et al., 2022). This reanalysis combines information from atmospheric models (the ERA-40 reanalysis from 1958 to 2002, the model ARPEGE since 2002) and in situ meteorological observations.

To study climate trends, we used the ADAMONT data (Verfaillie et al., 2017), which provides climate runs based on different pairs of global climate models (GCMs, CMIP5) and regional climate models (RCMs) in Europe (EURO-CORDEX initiative) (Jacob et al., 2014). The ADAMONT data is based on quantile mapping during the historical period (1950-2005) (Jakob Themeßl et al., 2011; Maurer and Pierce, 2014), and the reference on this period is the SAFRAN reanalysis. The climate projections (2005-2100) are available for three Representative Concentration Pathways (RCPs) (Van Vuuren et al.,



2011): RCP8.5, RCP4.5 and RCP2.6. Similar to Bonsoms et al. (2025), we investigated only two greenhouse gas emission scenarios: RCP4.5 and RCP8.5, excluding RCP2.6 because it is available only for a few pairs of GCM/RCM models. Overall, 200 we used 18 GCM/RCM pairs that were adapted locally using ADAMONT quantile mapping. These pairs provide weather data over the historical period and for the two emission scenarios (see details in Tab. 1).

GCM RCM	CNRM-CM5	EC-EARTH	HadGEM2	MPI-ESM-LR	NorESM1	IPSL-CM5A
ALADIN53	1950-2100					
ALADIN63	1950-2100					
CCLM4-8-17	1950-2100	1950-2100	1981-2099	1950-2100		
RACMO22E	1950-2100	1950-2100	1981-2099			
RCA4	1970-2100	1970-2100	1981-2099	1970-2100		1970-2100
REMO019				1950-2100		
HIRHAM5					1951-2100	
WFR331F						1951-2100
WFR381P						1951-2100

Table 1. Selected GCM/RCM model pairs and their associated time-period. These pairs are defined for two RCPs: RCP4.5 and RCP8.5.

2.3.2 Snowpack simulations and derived avalanche formation proxies

The meteorological data are used as input for the Earth continental surface model SURFEX. The soil model is ISBA (Decharme et al., 2011). The snowpack model is the detailed model Crocus (Vionnet et al., 2012). We used a 10-year spin-up to obtain 205 realistic initial conditions at the start of the simulation period. Crocus reproduces the evolution of the snowpack stratigraphy during the winter and the surface conditions continuously throughout the year. This wealth of data (up to 50 layers, each described by at least 5 variables, at a 3-hour resolution, on 5 elevation bands, and 4 aspects) must be reduced to construct a feature array and avoid overfitting (Ying, 2019).

The release of an avalanche can be formally classified into five avalanche problems (European Avalanche Warning Services (EAWS), 2022): new snow, wind slab, persistent weak layers, wet snow and gliding snow. The machine learning model must predict all avalanches, regardless of the avalanche problem. Therefore, it is essential to construct predictors that reflect this diversity. For each day, for a given aspect sector, we compute 115 physically sound features (Tab. 2) as follows:

- 215 – *New snow* (28 predictors): The primary driver of avalanche events is the amount of new snow. We characterized it by the depth of new snow accumulated over the past 24, 72, and 120 h at all the studied elevations. To quantify the intensity of solid precipitation, the mean and maximum snowfall rates over the last 24 and 48 h are also included as predictors.
- *Wind slab* (32 predictors): the occurrence and magnitude of snow drift are mainly driven by the wind speed and the characteristics of the snow surface (Mott et al., 2010). Wind speed must exceed a critical threshold velocity to initiate



220

wind-blown snow. The mean and maximum wind speed over the last 24 and 72 h are thus used as features. Wind direction is also used as a predictor to account for preferential deposition and erosion (with four dummy variables for North, West, South, and East components). Moreover, snow cohesion affects its wind-erodibility. We use the surface penetration depth of the Rammsonde as a proxy for the propensity of snow to be transported. We arbitrarily choose one elevation (2700 m) to limit the number of these predictors.

225

– *Persistent weak layers* (6 predictors): these problems are related to the presence of a weak layer in the pre-existing snowpack. The strength-stress ratio S_n (Roch, 1966) compares the shear strength of one layer to the shear stress due to

230

the overlying snowpack. This ratio is used to detect slab avalanche-prone situations (e.g. McClung, 1981; Reuter et al., 2022; Viallon-Galinier et al., 2023). We used the minimum values of S_n across defined depth intervals: 0.3 m bins from 0.2 m (similar to Reuter et al. (2022)) to 1.7 m, and one additional bin for depths >1.7 m. This predictor is computed only for the highest elevation (2700 m), as it is mainly involved in the release process.

235

– *Wet and gliding snow* (44 predictors): Mitterer and Schweizer (2013) showed that the release of wet avalanches is related to the snowpack liquid water content and the thickness of the snowpack that isothermal and/or wet. We defined the snowpack liquid water content ratio r as the ratio of liquid water content to snow water equivalent. We used the maximum values of r on the last 24 h and 72 h and its temporal evolution ($r_d - r_{d-24h}$, $r_d - r_{d-72h}$, $r_d - r_{d-168h}$) as predictors. We also added the liquid precipitation rate as a predictor.

240

– *General* (5 predictors): The number of avalanches is related to the number of avalanche paths in the considered domain. For instance, in Haute-Maurienne, only 14 avalanche paths face West and 36 paths face North. This number is thus added to the predictor list. Total snow depth is also an important predictor. For instance, a heavy snowfall at high elevation on a snow-free ground may not lead to a substantial avalanche flow. This last variable is relevant for all avalanche problems.

245

Note that the goal here is not to define the best predictors of avalanche formation, in general. The idea is to span different avalanche situations to achieve a sufficient predictive power with a limited number of features. In addition, the presented classification of features into avalanche problems is somewhat arbitrary, as some variables may be associated with multiple problems.

2.4 Machine learning model

2.4.1 Machine learning algorithm

Most comparable studies (Sielenou et al., 2021; Mayer et al., 2022; Viallon-Galinier et al., 2023; Hendrick et al., 2023) used the random forest algorithm. This method aggregates predictions from numerous independent decision trees. The extreme gradient boosting (XGBoost) algorithm (Chen and Guestrin, 2016) is another learning method based on decision trees. Unlike Random Forests, which build multiple independent trees in parallel, XGBoost constructs trees sequentially, where each new tree corrects the errors of the previous ones. Unlike Random Forests, XGBoost uses a loss function that is explicitly minimized through gradient boosting. This technique iteratively reduces prediction errors by fitting new trees to the residuals of previous



Related avalanche problem	Predictor description	Selected time or period	Selected elevations	Number of predictors
General	Number of paths in the domain	Constant	Constant	1
	Snow depth (m)	At 18:00	All	4
New snow	Height of new snow (m)	Cumulated at 18:00 on last 24, 72 and 120 h	All	12
	Snowfall rate ($\text{kg m}^{-2} \text{s}^{-1}$)	Mean and max. on last 24 and 72 h	All	16
Wind slab	Wind speed (m s^{-1})	Mean and max. over the last 24 and 72 h	All	16
	Wind direction (4 dummy variables)	Mean over last 24 and 72 h	2700 m	8
	Ram surface penetration (m)	Max. over last 24 and 72 h	All	8
Persistent weak layers	Natural stability ratio (min. on 6 depth intervals)	At 18:00	2700 m	6
Wet and gliding snow	Liquid water content ratio	Max. on last 24 and 72 h and difference with previous 24, 72 and 168 h	All	20
	Wet snow thickness on snowpack top (m)	Max. on last 24 and 72 h	All	8
	Rainfall rate ($\text{kg m}^{-2} \text{s}^{-1}$)	Mean and max. on last 24 and 72 h	All	16

Table 2. Selected predictors per aspect sector. *All* elevations means 1800 m, 2100 m, 2400 m, 2700 m. We recall that one day d is defined between 18:00 UTC on day $d - 1$ and 18:00 UTC on day d .

250 trees. We used this model especially to benefit from a custom loss function that accounts for uncertainties in the observed release days (see Sect. 2.4.2). To predict the daily number of avalanches, we chose the regression variant of the XGBoost algorithm (implemented using the XGBoost Python package) rather than a classifier.

2.4.2 Explicit modeling of uncertainty regarding the release date

255 A loss function aims to compute the difference between the prediction (here the daily number of avalanches) and the observation at each step of the training process. We defined a custom loss function to account for the uncertainty in the release date of each observed avalanche. For each day, we calculate the largest time period associated with all the observed avalanches that could occur on that day. The number of avalanches predicted by the model during this period is then compared to the range of the number of avalanches (the exact number is often not known) that could have occurred during the same period. This process is illustrated in Fig. 4. In more detail, the loss function for day d is built as follows:

260 – We identify all the avalanches in the EPA dataset that could have occurred on day d . Each avalanche i is characterized by an uncertainty interval defined by two dates $d_{i,1}$ and $d_{i,2}$. We define $\Delta T = [d_{min}, d_{max}]$ as the interval spanning from the earliest $d_{min} = min_i(d_{i,1})$ to the latest $d_{max} = max_i(d_{i,2})$. If no avalanche is observed on day d , then ΔT consists only of the single day d . For instance, for $d = 25/12$ in Fig. 4, $\Delta T = [24/12, 29/12]$.



265 – We compute the range $[n_{min}, n_{max}]$ of the number of observed avalanches within the time window ΔT . For example, in Fig. 4, for $\Delta T=[24/12, 29/12]$, $n_{min} = n_{max} = 7$ avalanches. Similarly, for $\Delta T=[13/12, 16/12]$, $n_{min}=2$ and $n_{max}=4$, depending on the triggering day of the avalanches associated with the paths 73144202 and 73040020.

– We compute the sum of the daily predicted number of avalanches over ΔT .

– We compute the signed distance between this predicted value and the interval $[n_{min}, n_{max}]$. This distance is then normalized by the length of ΔT (in days), and the resulting value is defined as the residual R .

270 The details of the chosen XGBoost hyper-parameters are provided in Appendix A for reproducibility.

2.4.3 Derived indicators of avalanche activity

The model predicts the daily number of avalanches for each aspect sector. To investigate trends in avalanche activity, we defined three indicators that quantify the avalanche activity at different time scales over the whole domain (i.e., we sum the number of simulated avalanches for all four aspect sectors):

275 – the number of avalanches per winter season (September to May). Winter seasons will subsequently be denoted solely by the year in which they begin; for example, winter 2020–2021 will be denoted as 2020.

– the number of avalanches per month.

– the maximum number of avalanches that occur during one rolling week for each year. This indicator reflects the magnitude of the largest avalanche cycle each year, assuming that large cycles are associated with a high number of avalanches.

280 To investigate changes in high values of this indicator, we fit non-stationary Generalized Extreme Value (GEV) distributions (Coles, 2001) on the data, and investigate the 30-year return level (i.e., the level associated with a 30-year return period). The application of this framework is detailed in Appendix B.

To assess temporal trends in these indicators and to fit the GEV distributions, we employed the Bayesian statistical framework implemented in the PyMC Python library (Abril-Pla et al., 2023). This approach enables us to incorporate prior knowledge and 285 compute the full posterior distributions of the parameters, including their uncertainties, which proved useful for many related avalanche problems (e.g., Eckert et al. (2010c); Fischer et al. (2020)).

2.4.4 Model evaluation

The model is evaluated on the mean absolute errors (MAE) of these three indicators during the reanalysed period 2006–2023. As in Viallon-Galinier et al. (2023), we used a "leave-one-year-out" (LOYO) evaluation method: each winter of the studied 290 period is, in turn, treated as a test set, with a model trained on the remaining winters.

To assess the benefits of our new method, we trained four versions of the model.

– $M_{d_1-d_2}^{2006-2023}$ was trained on the 2006–2023 period of the reanalysis and accounts for the uncertainties in the triggering date by using the custom-loss function described in 2.4.2.

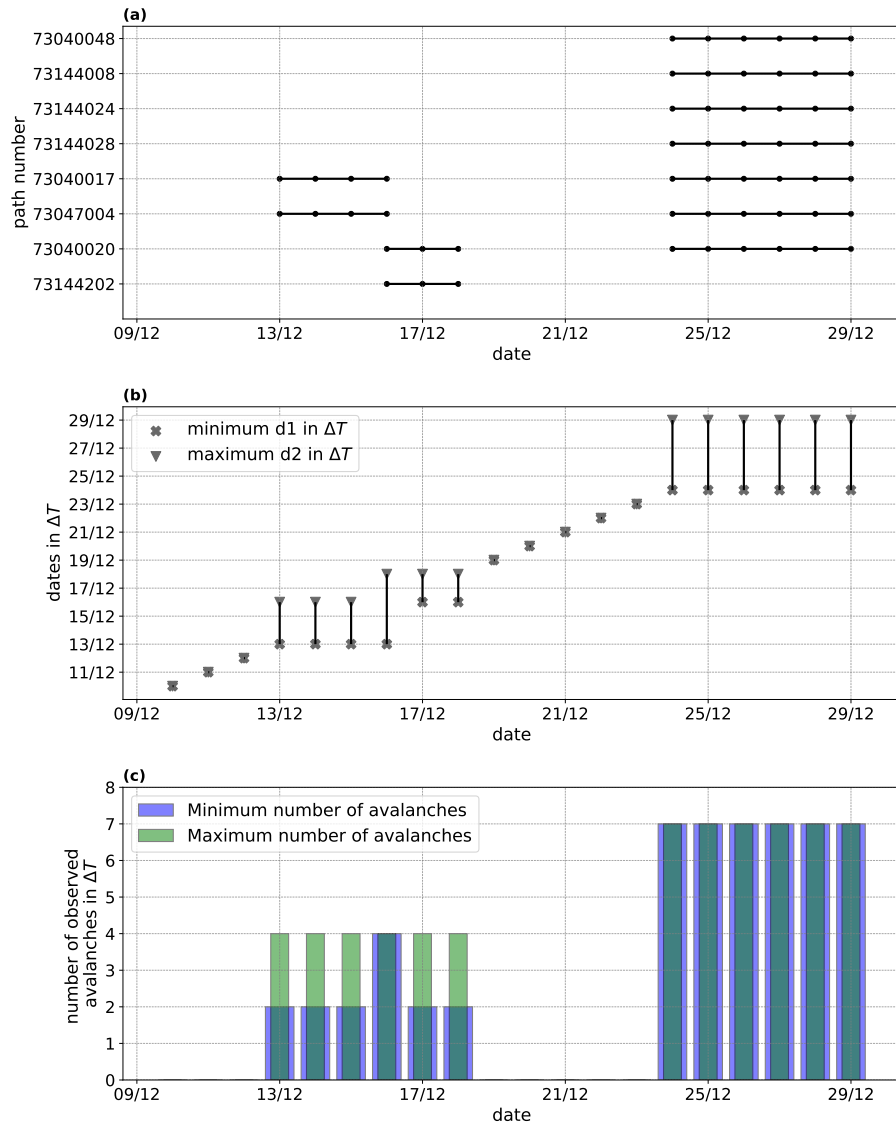


Figure 4. Illustration of the custom loss-function used in the training process, taking the example of the avalanches recorded in the Southern aspect sectors between the 10/12/2019 and the 29/12/2019. (a) Avalanches reported in the EPA dataset. Each continuous line corresponds to an avalanche, and each point represents a potential day for one avalanche. (b) Time-period ΔT corresponding to each date. (c) Minimum and maximum number of avalanches observed during the time-period ΔT associated to each date.



– $M_{d_1-d_2}^{1960-2023}$ was trained on the 1960-2023 period and accounts for the uncertainties in the triggering date.

295 – $M_{d_2}^{2006-2023}$ was trained on the 2006-2023 period and uses the default loss function of XGBoost and assumes that each avalanche occurred at the end of its period of uncertainty.

– $M_{d_2}^{1960-2023}$ was trained on the 1960-2023 period and uses the default loss function of XGBoost.

Using a similar approach, Viallon-Galinier et al. (2023) trained their models on the 1960-2018 period, assuming that each avalanche occurred at the end of its period of uncertainty. In the four models investigated here, we used the same features
 300 computed from the S2M reanalysis and the models were evaluated on the same winter seasons from 2006/2007 to 2022/2023.

3 Results

In the following sections, the four versions of the model are first evaluated over the 2006-2023 period. Then, the best one is used to correct the historical trend in avalanche activity between 1958 and 2023 based on the S2M reanalysis. Finally, we compute 1950-2100 trends from climate simulations.

305 **3.1 Model evaluation between 2006 and 2023**

We first evaluate the four versions of the model between 2006 and 2023 (Table 3). Accounting for both observation uncertainties and potential observation bias before 2006 reduces prediction errors. The annual MAE is reduced by half (from about 50 avalanches to 28 avalanches per year), the seasonal MAE by 3 (from about 5 avalanches to 1.4 per month) and the worst week MAE by half to one third (from 10-18 avalanches to 8 avalanches per week). Thus, the relevance of the modeling choices is
 310 confirmed, as they substantially improve the methodology and lead to the best scores on the three metrics.

Model version	Training period	Uncertainties on the triggering date	Annual MAE	Monthly MAE	Worst week MAE
$M_{d_1-d_2}^{2006-2023}$	2006-2023	taken into account	28.6 (23.4%)	1.4 (10.2%)	7.8 (21.6%)
$M_{d_1-d_2}^{1960-2023}$	1960-2023	taken into account	46.7 (38.2%)	5.2 (38.3%)	13.8 (38.3%)
$M_{d_2}^{2006-2023}$	2006-2023	not taken into account	51.3 (42.0%)	5.1 (37.8%)	10.6 (29.3%)
$M_{d_2}^{1960-2023}$	1960-2023	not taken into account	46.7 (38.2%)	5.0 (36.8%)	18.6 (51.9 %)

Table 3. Scores for the four models. The mean absolute errors correspond to a number of avalanches. The values in brackets are percentages calculated from the average value of each indicator. The model in bold is the one selected for the rest of this study.

The predictions of the model $M_{d_1-d_2}^{2006-2023}$ are detailed in Fig. 5. We recall that these predictions are generated with the leave-one-year-out method (see Sect. 2.4.4). The inter-annual variability of the number of avalanches per year (between about 40 and 500) is well predicted by the machine learning model (Fig. 5a, b). The model correctly identifies specific years, such as winter 2017/2018 with a record-breaking number of avalanches, and 2010/2011 with very low avalanche activity. The mean
 315 absolute annual error is 28.6 avalanches per year (23% of the mean number of avalanches per winter season). The bias is small:

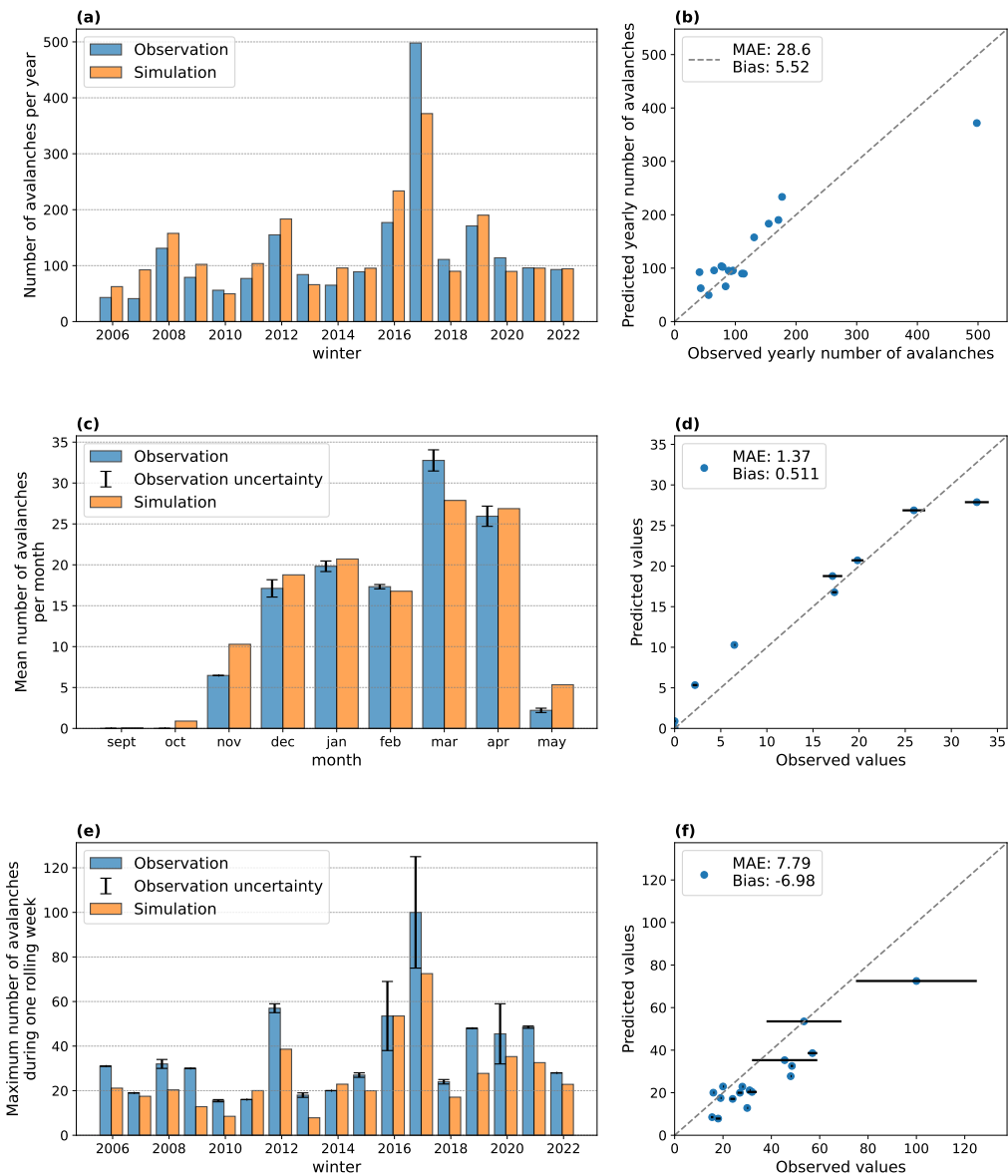


Figure 5. Evaluation of the model $M_{d_1-d_2}^{2006-2023}$ using the LOYO method on the annual number of avalanches (a, b), the mean number of avalanches per month over the 17 winter seasons (c, d), and the maximum number of avalanches during a week per winter season (e, f). The MAE and the bias are computed using the distance to the interval associated with the uncertainties (error bars on observations).



5.5 avalanches (4.5% of the mean number of avalanches per winter), showing that the error is almost centered on zero. The model is also capable of reproducing the average number of avalanches per winter month (Fig. 5c, d). There are almost no avalanches predicted or reported before November. Then the number of avalanches progressively rises until the peak activity in March. Avalanche activity almost disappears in May. The mean absolute monthly error is approximately 1.4 avalanches (10.4 % of the mean number of avalanches per month during the winter season), with a small bias of 0.5 avalanches. Focusing on the maximum number of avalanches during one rolling week per season (Fig. 5e, f), the mean absolute error is approximately 7.8 avalanches, representing 21% of the mean value. The model correctly predicts the inter-annual variability, but systematically underestimates the maximum number of avalanches per week, by around 20% over the entire period, as shown by a negative bias of -7.0 avalanches for the most active week of the year. All in all, the results show that the model performs well at annual and monthly scales and satisfactorily at the most active weekly scale. This demonstrates that the model is suitable for investigating climate-driven trends in these avalanche activity indicators.

3.2 1958-2023 reanalysis

A single XGBoost model is trained using all the winter seasons from 2006/2007 to 2022/2023. The model is then applied using the S2M reanalysis dataset from 1958 to 2023 as input data. The predicted daily number of avalanches is used to derive the three previously defined indicators of avalanche activity (Fig. 6). In addition, we compute the temporal linear trends of these indicators using a Bayesian framework (Abril-Pla et al., 2023). The linear trends are systematically expressed in % per decade relative to the 1974-2004 climatology, with its median value and the 10th–90th percentile posterior credible interval.

The predicted number of avalanches per winter season shows large inter-annual variability but an average decreasing trend (Fig. 6a). For instance, years with more than 200 avalanches are rather frequent (approximately every three years on average) before the late 1980s and become rare thereafter (only two occurrences in winter 1994-1995 and 2017-2018). The winter 2017-2018 appears to be the most intense in the 1958-2022 period. As expected, the trends from the raw observations are completely off from these assessments, which highlights that raw observations over a long period may be affected by sampling biases. Quantitatively, our model predicts a mean decreasing linear trend of -6.0% per decade in the annual number of avalanches over the period 1958–2023, with a 10th–90th percentile credible interval ranging from -11.4% to -0.8% (Appendix Fig. A1).

The decrease of the annual number of avalanches is not uniform during the winter season as shown by contrasting 30-year periods at the beginning and at the end of the dataset: 1958–1988 and 1993–2023 (Fig. 6b). For instance, the resulting trends indicate a median slope of -4.7% (with a credible interval ranging from -10.2 to +0.9%) per decade in the avalanche activity in December, January, and February (DJF) and of -8.5% (between -13.4% and -3.5%) per decade in March, April and May, with a peak at -15.4% for the April avalanche activity (Appendix Fig. A1). Therefore, the decrease in avalanche activity in the past has been greater in spring than in winter.

The weekly maximum number of avalanches for each winter season is shown in Fig. 6(c). As we use a Bayesian framework to fit the GEV distribution on the data, the slope distribution of the return levels is directly provided within the inference procedure. The results show a decreasing slope of the 30-year return level by -3.5% (between -8.4% and +1.2%) per decade relative to the mean return level between 1974 and 2004. This downward trend is less significant than the one observed in the

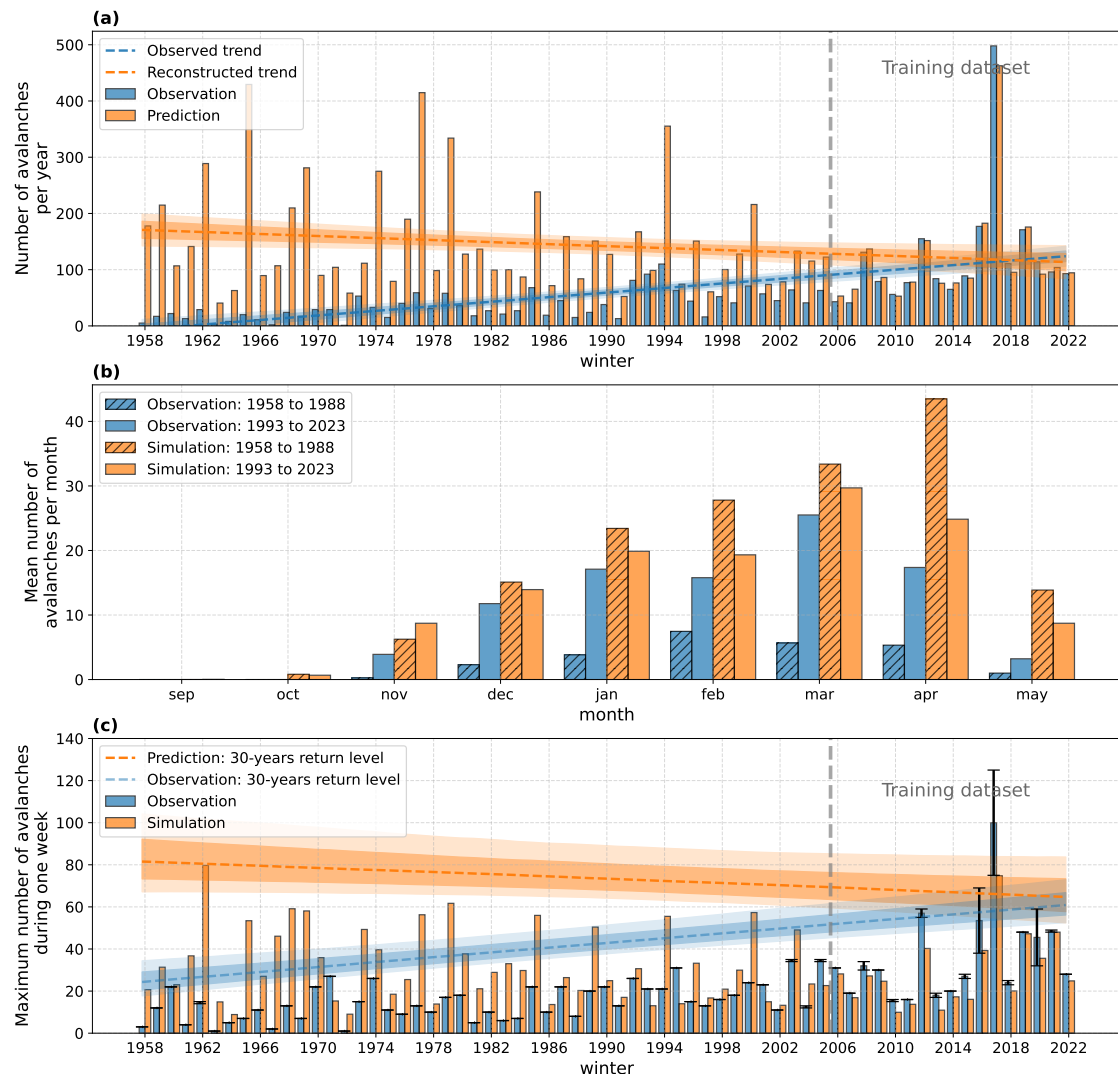


Figure 6. Past avalanche activity: a) annual number of avalanches, b) mean number of avalanches per month, c) maximum number of avalanches per week. The model predictions are shown in orange. The raw observations are shown in blue. For a) and c), linear trends are represented with their 10, 25, 50, 75, 90th percentiles.

350 total number of avalanches, suggesting that the magnitude of large cycles has decreased at a lower rate than the total number of avalanches.



3.3 1950-2100 climate simulations

The same machine learning model is applied to all members of the climate simulations (18 per scenario), and the avalanche activity is quantified by the three previously defined indicators. In contrast to the single reanalysis, the linear trends derived from 355 climate simulations for a given scenario are not only made uncertain by the inter-annual variability but also by the inter-model variability. To compute the probability distribution function of the trend slope, we arbitrarily assumed that all GCM/RCM pairs are equiprobable and evaluated the overall credibility interval by pooling posterior samples derived from individual projections (see Appendix Fig. A1).

The annual number of avalanches clearly shows a decreasing trend under advanced climate change and its consequences for 360 snowpack characteristics (Fig. 7a). The mean number of avalanches in the historical simulations is around 25% higher than that in the reanalysis. However, the trends are similar with a historical decrease at a median rate of -5.5% per decade, but with large uncertainties (10th–90th percentile posterior credible interval ranging from -16.4% to 8.1%). The projections for the 21st century show a decrease in the annual number of avalanches at median rates of -4.6% per decade for the RCP4.5 scenario and -8.8% for the RCP8.5 scenario with respect to the 1974–2004 period. The associated uncertainties are shown in Table 4. In 365 other words, the results indicate a reduction of approximately 37% (respectively 65%) in the mean number of avalanches over the 2070–2100 period compared with the 1974–2004 baseline in the RCP4.5 scenario (resp. RCP8.5).

The expected decline of avalanche activity is heterogeneous between seasons (Fig. 7b). First, the higher number of avalanches predicted by historical climate simulations compared to the reanalysis mainly arises from stronger activity in March and April, while DJF avalanche activity is broadly consistent between the two datasets. Then, the projected DJF avalanche activity appears 370 almost unaffected by climate change, except for the RCP8.5 at the end of the century. Conversely, a marked decline in avalanche activity is expected in March, April, and May (MAM) for all scenarios. The projected decrease in the annual number of avalanches is thus primarily driven by the strong reduction in spring avalanche activity. For instance, the number of avalanches in DJF is expected to decrease only by 3.3% per decade under RCP4.5 and by 6.6% per decade under RCP8.5, while in MAM, the expected decreases correspond to 5.4% per decade under RCP4.5 and 10.1% per decade under RCP8.5, 375 relative to the 1974–2004 reference period (Table 4). April was historically one of the most active months for avalanches; however, under the RCP8.5 scenario, by the end of the century, avalanche activity in April is projected to be very limited. Similarly, in May, avalanche activity is expected to be nearly absent under both scenarios, indicating a substantial shortening of the avalanche season.

It is projected that there will be a decrease in the amplitude of large avalanche cycles by the end of the century, with a 380 lower rate for RCP4.5 and a higher rate for RCP8.5 (Fig. 7c). Yet, considering the credible intervals, for the near future (2020–2050) or under the RCP4.5 scenario at all temporal horizons, large avalanche events with intensities comparable to those observed during the 1974–2004 reference period remain possible with a similar probability. Indeed, the 30-year return levels show respective trends of -1.8% and -4.6% per decade for the RCP4.5 and RCP8.5 scenarios relative to the mean return levels computed from the historical runs between 1974 and 2004. In other words, the 30-year avalanche cycle is expected to

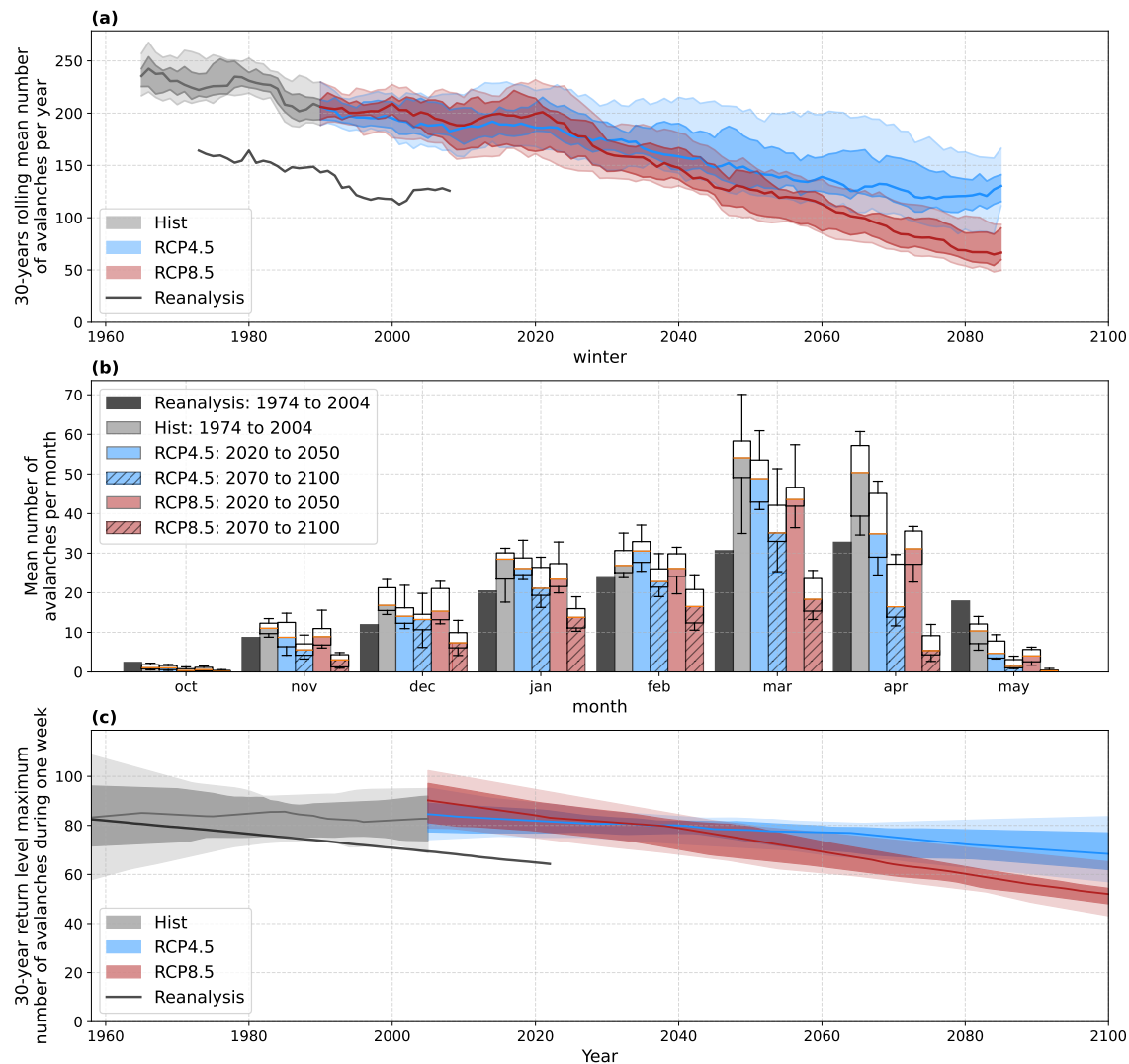


Figure 7. Climate simulations of avalanche activity: a) 30-year running mean of the annual number of avalanches, b) mean number of avalanches per month over different periods and c) 30-year return level of the maximum number of avalanches per week.

385 be composed of approximately 15% (resp. 35%) fewer avalanches in 2100 compared to the 1974-2004 reference period in the RCP4.5 scenario (resp. RCP8.5).



	RCP4.5: 2005–2100 (% per decade)	RCP8.5: 2005–2100 (% per decade)
Annual number of avalanches	-4.6 [-8.9, -0.8]	-8.8 [-12.3, -5.6]
Number of avalanches in DJF	-3.3 [-8.1, 1.1]	-6.6 [-11.4, -2.0]
Number of avalanches in MAM	-5.4 [-11.0, -1.6]	-10.1 [-14.1, -7.0]
30-year return level of the maximum number of avalanches during one week	-1.8 [-5.7, 2.0]	-4.6 [-8.0, -1.3]

Table 4. Median values and 10th–90th percentile posterior credible interval associated with the slope of the avalanche activity indicators in % per decade with respect to the 1974–2004 period. The associated ensemble distributions are represented in Appendix Fig. A1.

4 Discussion

4.1 Methodology

This work uses a new methodology compared to previous studies to investigate future changes in avalanche activity by using a regressor and considering two key aspects of the training dataset: the heterogeneity of observations over time and uncertainties associated with triggering dates.

First, using a machine learning regressor algorithm enables us to progress beyond studies that used binary classifiers. To our knowledge, all studies that predict daily avalanche activity from snow stratigraphy using machine learning methods rely on classification algorithms to predict whether a day is avalanche-prone (Mayer et al., 2024; Viallon-Galinier et al., 2023; Hendrick et al., 2023; Kronholm et al., 2006), or to categorize daily avalanche activity into three classes: null, moderate, or high (Sielenou et al., 2021). These models do not provide quantified information about the magnitude of avalanche activity during the avalanche days, and are mainly used for short-term avalanche hazard forecasting and for pre-detecting situations that may require specific attention by the forecaster. Their predictions generally show high recall but low precision: most observed avalanche days are well predicted, but the predictions may contain many false alarms. Using a regressor thus allows us to predict the daily number of avalanches and to quantify climate trends in avalanche activity using different indicators, without treating all avalanche days equally. However, the number of avalanches gives no information on the size of avalanches and the potential damage: many small avalanches may have no impact at all, while a small number of large ones could cause significant damage. Future research could investigate additional target variables, such as deposit volume (Kern et al., 2020), to enhance the scope of potential applications. In addition, we may improve our regressor algorithm. Indeed, the distribution of the observed daily number of avalanches corresponds to a zero-inflated regression count data configuration, characterized by integer values with an over-representation of zeros (Young et al., 2022). We did not use a specific model to handle this distribution. More complex models adapted to zero-inflated count data Fávero et al. (2024), such as a two-stage model that combines a classifier and a Poisson regressor, might improve the methodology (e.g. Orhobor et al., 2023; Rožanec et al., 2023). In such a framework, the GEV component would need to be formulated using a discrete extreme value distribution, as proposed by Evin et al. (2021).



410 In the present study, it relies on a continuous GEV formulation as the model predicts continuous daily numbers of avalanches. Moreover, the model tends to underestimate the most active week of the year (Fig. 5e), indicating limitations in its ability to predict extreme avalanche activity. Combining a similar machine learning framework with an extreme value approach could help better represent the tail behavior of the distribution and improve the credibility of predicted extremes (Evin et al., 2021).

415 Secondly, to address heterogeneity in past observations, we trained a machine learning model using the EPA dataset between the winter seasons 2006/2007 and 2022/2023. We have shown that training the model on a larger time period (Tab. 3), as done in (e.g. Viallon-Galinier et al., 2023; Sielenou et al., 2021), leads to lower scores. Besides, the predicted number of 420 avalanches based on the reanalysis significantly deviates from the observations in the distant past (Fig. 6). These results suggest that avalanche sampling was not constant in the Haute-Maurienne valley over the entire 1958–2023 period, with greater uncertainty in the early portion of the time series. While this result is specific to the studied area, it confirms that the EPA dataset, as with most avalanche records stemming from human observations or archives, should be used with caution when 425 considering the distant past (Giacona et al., 2021). However, training the model on a smaller dataset also has its drawbacks. In particular, the approach implicitly assumes that the range of snow conditions encountered during the model application period (1950–2100) is represented within the training dataset (2006–2023). This assumption becomes more plausible as the length and diversity of the training period increase. When the model is applied to conditions outside the range of its training data, its 430 predictions are likely to be unreliable. In other words, the model cannot handle new, unknown avalanche situations and only predicts the future probability of situations that have already occurred. This limitation is particularly critical when analyzing extreme avalanche cycles. In this regard, including the 2017/2018 winter season—characterized by exceptionally unusual snow conditions—within the training dataset is especially valuable. To overcome this limitation, physics-based avalanche models (Durand et al., 1999; Reuter et al., 2022) may help this machine learning approach handle new conditions not encountered during training.

435 Thirdly, we showed that accounting for the uncertainties in the release dates in the training step significantly improves the prediction scores (Tab. 3). This was achieved through the use of a custom loss function in the XGBoost algorithm. This approach enabled us to accurately associate daily snow conditions with the corresponding avalanche activity without making any assumptions about the exact triggering dates. Standard random forests widely used in the literature (e.g. Mayer et al., 2022; Viallon-Galinier et al., 2023; Sielenou et al., 2021) do not allow for the integration of uncertainties through a loss function.

4.2 Input data

440 The results are strongly influenced by the quality of the input data, specifically the avalanche observations and associated predictors. Enhancing the quality of these data sources may lead to improved outcomes. Furthermore, as this study is limited to a single location and utilizes high-quality data, additional research is necessary to determine whether these findings can be generalized to other regions.

The avalanche activity described in this paper corresponds to the one reported by the EPA, which is not representative of all the avalanches that can occur, particularly those at higher altitudes that do not reach the EPA thresholds (Fig. 1). Nevertheless, these avalanches can still pose a threat to snow recreationists. In addition, the EPA thresholds of the studied area are located



within a relatively narrow elevation range, and we assumed that avalanche activity is driven by snow conditions aggregated over
445 all the elevation bands between 1800 m and 2700 m. As a result, the influence of elevation on temporal trends in avalanche
activity cannot be explicitly isolated in the present analysis. This limitation is noteworthy, as elevation has been shown to
play a major role in governing snowpack evolution and long-term changes in avalanche activity, particularly in the context of
climate change (Eckert et al., 2024). Moreover, this study is specific to the Haute-Maurienne valley, characterized by numerous
450 recorded avalanches. The exact same methodology is not applicable in other areas where the too small number of recorded
avalanches does not yield a sufficient training data set. Working on model transferability (Wang et al., 2022) or by reasoning
at alternative spatial scales (e.g. considering individual avalanche paths and accounting for their topographical specificity by
adding topographic properties in the features) could further strengthen the methodology and facilitate its application to other
locations.

The model is trained on weather and snow predictors derived from the S2M reanalysis at the massif scale. In the Haute-
455 Maurienne valley, snowfall is highly influenced by specific meteorological events (easterly return flows) that can produce
substantial localized accumulation near the Italian border while nearby areas receive minimal snowfall, as exemplified by
the large 2008 avalanche cycle in Southeast France (Eckert et al., 2010b). Consequently, the snowpack simulations cannot
fully capture this heterogeneity and may yield locally unrepresentative conditions. Nevertheless, as these issues are present in
460 both the training and application datasets, there should still be a predictive relationship between simulated meteorological and
snowpack conditions and avalanche activity. Besides, the S2M reanalysis is also subjected to biases that can vary with time,
which affects reanalysed climatic trends (Vernay et al., 2022): the number of assimilated observations varies over time and
the meteorological conditions are simulated by the ERA40 model (Uppala et al., 2005) before 2002 and by the operational
forecasts of the French global NWP model ARPEGE thereafter. In addition, we assumed here that avalanche hazard evolution
465 is solely controlled by changes in snow cover. However, avalanche activity can also be impacted by changes in land use, such
as land abandonment and reforestation (Mainieri et al., 2020; Zgheib et al., 2022; Moen et al., 2004). The projected reduction
of avalanches may also initiate a positive feedback loop: fewer avalanches may increase the density of small-diameter trees in
avalanche starting zones, reducing future avalanche magnitudes even more (Teich et al., 2012).

The climate trends computed in this study are based on the ADAMONT framework, which relies on a projection onto a
massif-elevation grid of RCM simulations and on an advanced quantile mapping with the reanalysis on the historical period
470 (Verfaillie et al., 2017). The EURO-CORDEX Regional Climate Model Ensemble simulations are generally too cold and too
wet (Matiu et al., 2024; Vautard et al., 2021; Smiatek et al., 2016). The ADAMONT method is designed to reduce systematic
discrepancies between climate model outputs and the reference reanalysis. However, in high-mountain environments, the
correspondence between regional climate model grid points and the associated reanalysis points is challenging due to strong
elevation gradients and complex topography. Furthermore, the ADAMONT bias-correction procedure is applied independently
475 to each elevation band, without explicitly enforcing vertical coherence among corrected variables. This approach may therefore
disrupt altitude-dependent physical relationships and introduce inconsistencies across elevations. These limitations are further
amplified near the rain–snow transition zone, where strong non-linear responses to small temperature biases can generate significant
biases in snow-related variables. Indeed, in the Haute-Maurienne valley at 2700 m, the mean winter snow depth is



still around 30% higher in ADAMONT climate simulations than in the reanalysis (not shown), which may explain why the
480 avalanche activity computed from historical ADAMONT simulations is significantly higher compared to one computed from the reanalysis (Fig. 7). A strong assumption of quantile mapping is also the temporal stationarity of the bias, which remains questionable under pronounced climate change (Verfaillie et al., 2017). As a result, we based our analysis on climatic trends (in % per decade) rather than absolute values, which are more prone to systematic biases. Moreover, Cannon et al. (2015) analyzed the impact of bias correction via quantile mapping on extreme precipitation and concluded that quantile mapping can inflate the
485 magnitude of relative trends in precipitation extremes with respect to the raw dataset. A specific treatment of extreme values is used in ADAMONT: for RCM values greater than the 99.5% quantile, the quantile mapping method is not applied and a constant adjustment is applied to allow for new extremes (Verfaillie et al., 2017). This treatment of the extreme values might be better than a simple quantile mapping method, but may be insufficient to capture the correct trends in the extreme values. Future work should therefore focus on more advanced extreme-value frameworks to better constrain the upper tail and assess
490 the robustness of the projected changes in the extreme events.

4.3 Climate trends in avalanche activity

The past trend in avalanche activity based on the S2M reanalysis (1958–2023) shows a decrease in the mean annual number of avalanches between 1958 and 2023, at a rate of approximately 6% per decade. Based on the S2M reanalysis and the raw
495 EPA dataset without any prior statistical pre-processing, Castebrunet et al. (2012) found no significant trend in avalanche occurrences at the scale of the Northern French Alps between 1958 and 2009. Using a more advanced statistical treatment of the EPA dataset, Eckert et al. (2013) found a decrease of 19% in the mean number of avalanches per winter between 1980 and 2009 in the entire French Alps, which corresponds to approximately 6% per decade, in line with our result. We also showed that the decrease in avalanche activity is more pronounced during spring, which is consistent with Reuter et al. (2025)
500 who reported an advancement of about three weeks of the onset date of wet-snow activity from 1958 to 2020. Moreover, we found that the magnitude of large avalanche cycles, quantified by the maximum number of avalanches during one week, decreased by around 3.5% per decade, at a lower rate compared to the annual number of avalanches. Peitzsch et al. (2021) used dendrochronology analysis in the Rocky Mountains and demonstrated that the probability of large avalanche occurrence decreased by approximately 2% per decade from 1950 to 2017. Although this metric is not directly comparable to our results, since we analyze avalanche counts during one week rather than the occurrence of large avalanche, both metrics address changes
505 in the frequency of large avalanche cycles over time.

Regarding future climate simulations, our results are in agreement with the small number of existing studies that provide quantitative assessments, which consistently report a marked decrease in the mean annual avalanche occurrence. Mayer et al. (2024) reported a decrease in the number of avalanche days between the periods 1990–2020 and 2969–2999, with the magnitude of the decrease depending on station elevation. At the station with the lowest elevation (1824 m, similar to the
510 Haute-Maurienne valley floor), the number of avalanche days declined by approximately 30% under the RCP4.5 scenario and by about 60% under the RCP8.5 scenario. At higher altitudes, between 2300 m and 2800 m, this decline is less pronounced, reaching around 10% in the RCP4.5 scenario and 20 to 30% in the RCP8.5 scenario. Mayer et al. (2024) also showed that



seasonality in dry-snow avalanche activity, characterized by peaks in January and February, remains mostly unchanged. However, the seasonality of wet snow avalanches is expected to change: rather than starting in March as they did in the reference 515 period, these avalanches are expected to appear earlier in the season and decrease in number in April and May. Taking into account all avalanche problems, it leads to a significant reduction in spring avalanches. Similarly, in the Rocky Mountains, the wet avalanches are expected to start earlier than historical averages (around 40 to 45 days earlier in the high emission scenario) (Lazar and Williams, 2008). Our findings indicate a drop in the number of avalanches in April and May, especially 520 in the RCP8.5 scenario. This is consistent with our results, suggesting that the overall decrease may result from a shift of the wet snow activity from late season to the high winter, in line with what already occurred at low elevations (Giacona et al., 2021). We also found that the return levels of large avalanche cycles are expected to decrease, but at a slower rate than the mean avalanche activity. This is consistent with the results of Ortner et al. (2025), which show that despite climate change, 525 some locations continue to be at high risk of avalanches. Furthermore, Bonsoms et al. (2025) demonstrated that the mean daily snowfall in the Pyrenees at 2,500–3,000 m will decline significantly and emphasize that extreme snowfall events will change only slightly. Similarly, Le Roux et al. (2023) demonstrated that the expected decrease in the 100-year return level of daily snowfall is slower than the expected decrease in the mean annual maximum value. This illustrates that a decrease in mean 530 conditions does not necessarily imply a proportional decrease in extreme values.

The snowpack conditions in the Haute-Maurienne valley are rather specific: a relatively high valley floor compared to typical 535 alpine valleys and substantial precipitation associated with eastern flows. Therefore, the spatial generalization of these results should be addressed in future work. In particular, future analyses should explicitly account for the influence of elevation on avalanche activity, given its major role in modulating the impacts of climate change on snowpack conditions (Dumont et al., 2025) and extreme snowfall events (Le Roux et al., 2023). Based on documented changes at low elevations (Giacona et al., 2021) and high elevations (Ballesteros-Cánovas et al., 2018), a conceptual framework describing elevation-dependent 540 avalanche activity has been proposed by Eckert et al. (2024). However, further investigations are required to provide quantitative assessments of these elevation-dependent effects.

5 Conclusions

This study aims to better understand the impact of climate change on avalanche activity in the European Alps using an exemplary 545 alpine valley. This study brings methodological improvements and provides quantified trends for several indicators of avalanche activity.

This study focuses on the upper part of the Haute-Maurienne valley in the French Alps, a region offering several advantages 550 for the analysis of avalanche activity. In particular, it benefits from a long-term avalanche observation dataset documenting numerous events on well-identified avalanche paths over several decades, collected using a methodology that is as homogeneous as possible over time. To model avalanche activity, we combined meteorological and snowpack modeling, using the SAFRAN 555 reanalysis for past conditions and an ensemble of climate simulations for future projections, together with the Crocus snow-



545 pack model. This framework provides consistent meteorological and snowpack variables at the massif scale, which are used as predictors of avalanche activity.

This study introduces a machine learning regressor to predict the daily number of avalanches, going beyond previous works based on binary classification. Unlike classifiers, it provides insight into the magnitude of avalanche activity and enables the use of quantitative indicators for trend analysis. The model was trained only on post-2006 data to avoid biases from inconsistent 550 historical observation records, and the training step accounts for uncertainties in the reported avalanche release date, which significantly reduces prediction biases and errors. The proposed chain model is generic and can be transferred to other regions where simulated meteorological and snowpack data, together with systematic avalanche observations, are available.

This study shows a clear long-term decline in avalanche activity linked to climate warming. In the past, both reanalysis and historical climate simulations indicate a clear downward trend in the annual number of avalanches. The reanalysis exhibited 555 a trend of -6.0% per decade over the 1958–2023 period (1974–2004 baseline). In the climate historical simulations (1950–2005), the median trend is estimated at -5.5% per decade. This decline is seasonally heterogeneous, mainly driven by a sharp reduction in spring avalanches (March–May), while winter activity (December–February) remains relatively stable. The 30-year return level of weekly maximum avalanche activity shows a decline of -3.5% per decade for the reanalysis from 1958 to 2023. This suggests a moderate decrease in extreme avalanche events, although less pronounced than the decline in total 560 avalanche numbers. For the future, we used an ensemble of 18 GCM/RCM couples for the RCP4.5 and 8.5 emission scenarios.

The projected evolution of avalanche activity during the twentieth century is consistent with the historical decline observed between 1958 and 2005. Under RCP4.5 and RCP8.5 scenarios, the annual number of avalanches is expected to decrease by 4.6% and 8.8% per decade, respectively (relative to the 1974–2004 baseline). By the end of the century, this corresponds to a 37% reduction under RCP4.5 and 65% under RCP8.5 compared to 2025. Again, while winter activity remains relatively stable, 565 spring avalanches (March–May) are projected to nearly disappear, leading to a substantial shortening of the avalanche season. Extreme events also decrease, but at more moderate rates, with return levels expected to decrease by 1.8% and 4.6% per decade under RCP4.5 and RCP8.5 scenarios relatively to the 1974–2004 baseline.

Our results show a marked decrease in avalanche activity in the Haute-Maurienne valley, both in terms of frequency and intensity, particularly driven by a sharp reduction in spring avalanches. However, unlike lower-elevation ranges such as the 570 Vosges (Giacona et al., 2017)—where avalanche activity has nearly disappeared in the 20th century due to natural and anthropogenic warming—avalanches remain a frequent and significant phenomenon in the Haute-Maurienne. This highlights the persistence of avalanche risk in high alpine environments, even under ongoing climate change. Future work should explore how evolving snow and weather regimes may continue to reshape the spatial and temporal patterns of avalanche activity in mountainous regions.



575 **Appendix A: Hyper-parameters**

The gradient boosting model's optimal hyper-parameters depend on its predictors. The choice of hyper-parameters was informed by expert knowledge. For instance, the maximum depth of the trees was set to 6, the default value that prevents overfitting while maintaining sufficient model complexity. The *subsample* and *colsample by tree* parameters has been set to 0.7 and 0.8 respectively, to prevent overfitting. Regularization tends to reduce the predicted probability of rare events. Setting 580 *lambda* to zero allows the model to predict rare events. They are summarized in Table A1. Furthermore, the results show that the scores (defined in the next section) are not greatly affected by the chosen hyper-parameters, demonstrating that the model is robust.

Hyper-parameter	Selected value
max depth	6
eta	0.1
subsample	0.7
colsample by tree	0.8
alpha	0
lambda	0

Table A1. Hyper-parameters values chosen in the machine learning model

Appendix B: Generalized Extreme Value distribution

According to extreme value theory (Coles, 2001), the Generalized Extreme Value (GEV) distribution is the suitable model for 585 block maxima (e.g., annual maximum rainfall or here the annual maximum number of avalanches considered as a continuous variable). For example, if Y is a maximum over a block of one year, the probability that Y is below y is given by the following distribution:

$$P(Y < y) = \begin{cases} \exp \left\{ - \left[1 + \xi \left(\frac{y - \mu}{\sigma} \right) \right]^{-1/\xi} \right\}, & \text{for } \xi \neq 0, \\ \exp \left\{ - \exp \left(- \frac{y - \mu}{\sigma} \right) \right\}, & \text{for } \xi = 0. \end{cases} \quad (B1)$$

where:

590

- μ is the location parameter, determining the center of the distribution.
- σ is the scale parameter. This positive number controls the spread of the distribution.
- ξ is the shape parameter, governing the tail behavior.



595 This distribution cannot be applied directly to non-stationary processes, such as snow-related variables in a changing climate. To model such processes, a first approach consists in considering smaller time-windows over which the stationarity assumptions may hold, and compare the results over the different sub-periods. However this approach reduces the data quantity used for each GEV fit, resulting in significant uncertainties. We therefore chose another approach, which consists in defining the GEV parameters as functions of time. As done in Le Roux et al. (2022), we assumed that μ and σ vary linearly with time, while ξ is kept constant.

600 *Author contributions.* François DOUSSOT: Conceptualization, Data curation, Methodology, analysis, Visualization, Writing - original draft. Léo VIALLON-GALINIER: Supervision, Validation; Writing - review and editing. Nicolas ECKERT: Funding acquisition ; Writing - review and editing. Pascal HAGENMULLER: Funding acquisition, Supervision, Validation; Writing - review and editing.

Competing interests. The authors declare no competing interests.

605 *Acknowledgements.* This study heavily relies on the systematic observation of avalanches by the ONF/RTM and the EPA database maintenance by Inrae. In particular, we would like to acknowledge the two avalanche observers S. Filliol and D. Bois for observations in the 2006-2023 period in Haute-Maurienne. This research was co-financed by the European Union, European Regional Development Fund (FEDER) through the project QUAAACC. CNRM and IGE are members of Labex OSUG@2020. N. Eckert is member of the Grenoble Risk Institute (<https://risk.univ-grenoble-alpes.fr/en>) and acknowledges support from the French National Research Agency to the IRIMONT program (ANR-22-EXIR-0003).

610 *Data availability.* EPA data for France is publicly available at: <https://www.avalanches.fr/>. The S2M reanalysis is an open-access dataset available at <https://doi.org/10.25326/37v2020.2>

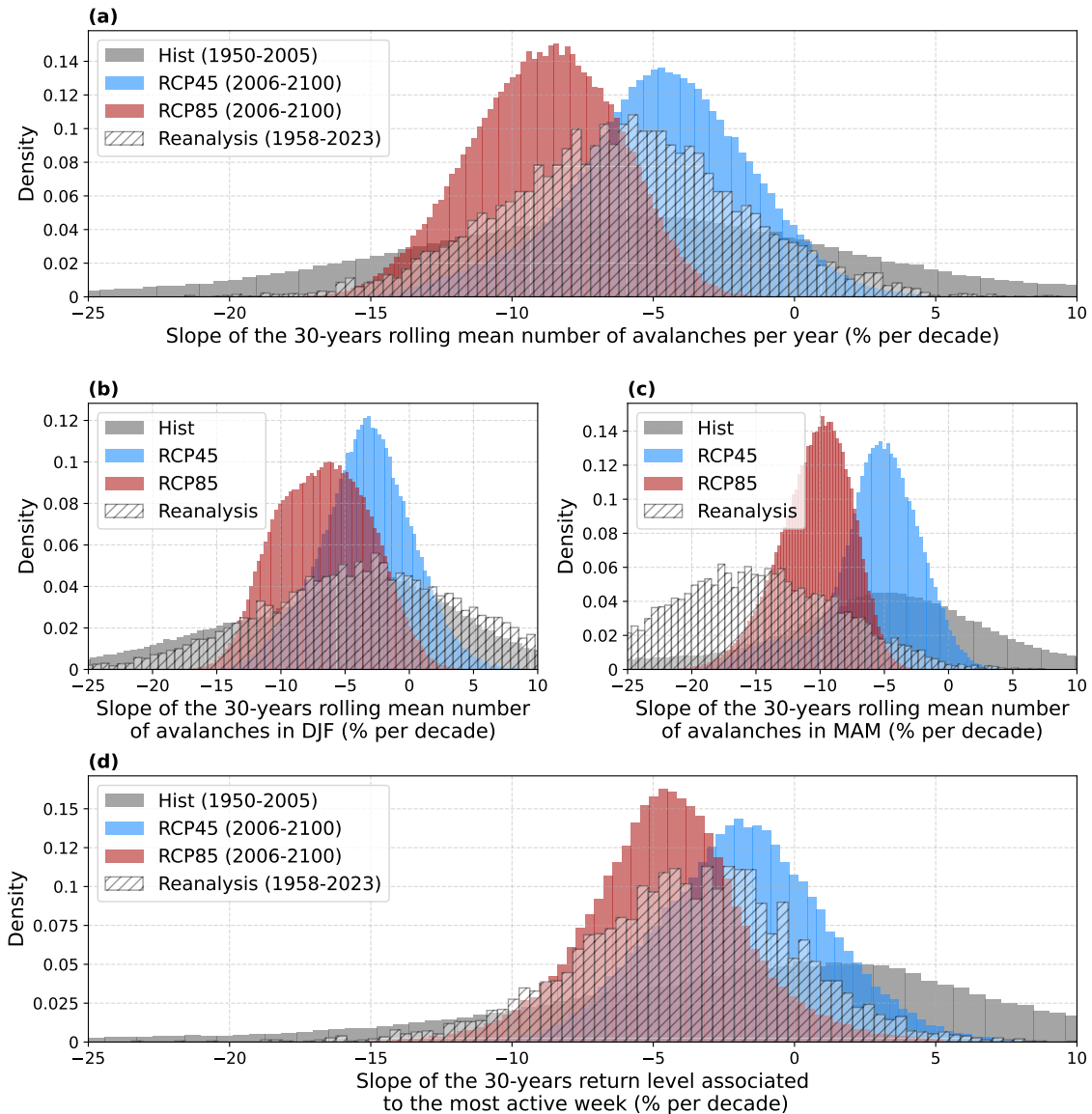


Figure A1. Distribution of the climatic trends based on ADAMONT simulations.

- (a) represents the distribution of the slope associated with the number of avalanches per year.
- (b) and (c) represent the distribution of the slope of the number of avalanches in December, January, and February (DJF) and March, April, and May (MAM).
- (d) shows the distribution of the slope relative to the 30-year return level corresponding to the maximum number of avalanches during 1 week.



References

Abril-Pla, O., Andreani, V., Carroll, C., Dong, L., Fonnesbeck, C. J., Kochurov, M., Kumar, R., Lao, J., Luhmann, C. C., Martin, O. A., Osthege, M., Vieira, R., Wiecki, T., and Zinkov, R.: PyMC: a modern, and comprehensive probabilistic programming framework in Python, *PeerJ Computer Science*, 9, e1516, <https://doi.org/10.7717/peerj-cs.1516>, 2023.

615 Ballesteros-Cánovas, J. A., Trappmann, D., Madrigal-González, J., Eckert, N., and Stoffel, M.: Climate warming enhances snow avalanche risk in the Western Himalayas, *Proceedings of the National Academy of Sciences*, 115, 3410–3415, <https://doi.org/10.1073/pnas.1716913115>, 2018.

Barkat, I., Lin-Kwong-Chon, C., Duclos, A., Carrel, M., Staehly, S., and Bourgeois, G.: OPTICAL MONITORING OF AVALANCHE REALEASE ZONES IN BESSANS, HAUTE MAURIENNE VALLEY, FRANCE, WITH A REMOTE AND ENERGY SELF-620 SUFFICIENT CAMERA SYSTEM, in: ISSW - International Snow Science Workshop, pp. 1041–1048, Tromsø, Norway, <https://hal.science/hal-04850783>, 2024.

Beniston, M. and Stoffel, M.: Rain-on-snow events, floods and climate change in the Alps: Events may increase with warming up to 4°C and decrease thereafter, *Science of The Total Environment*, 571, 228–236, <https://doi.org/https://doi.org/10.1016/j.scitotenv.2016.07.146>, 2016.

625 Bonsoms, J., López-Moreno, J. I., Lemus-Cánovas, M., and Oliva, M.: Future winter snowfall and extreme snow events in the Pyrenees, *Atmospheric Research*, 315, 107 912, <https://doi.org/https://doi.org/10.1016/j.atmosres.2025.107912>, 2025.

Bourova, E., Maldonado, E., Leroy, J.-B., Alouani, R., Eckert, N., Bonnefoy-Demongeot, M., and Deschartres, M.: A new web-based system to improve the monitoring of snow avalanche hazard in France, *Natural Hazards and Earth System Sciences*, 16, 1205–1216, <https://doi.org/10.5194/nhess-16-1205-2016>, 2016.

630 Bozzoli, M., Crespi, A., Matiu, M., Majone, B., Giovannini, L., Zardi, D., Brugnara, Y., Bozzo, A., Berro, D. C., Mercalli, L., and Bertoldi, G.: Long-term snowfall trends and variability in the Alps, *International Journal of Climatology*, 44, 4571–4591, <https://doi.org/https://doi.org/10.1002/joc.8597>, 2024.

Cannon, A. J., Sobie, S. R., and Murdock, T. Q.: Bias Correction of GCM Precipitation by Quantile Mapping: How Well Do Methods Preserve Changes in Quantiles and Extremes?, *Journal of Climate*, 28, 6938 – 6959, <https://doi.org/10.1175/JCLI-D-14-00754.1>, 2015.

635 Cappabianca, F., Barbolini, M., and Natale, L.: Snow avalanche risk assessment and mapping: A new method based on a combination of statistical analysis, avalanche dynamics simulation and empirically-based vulnerability relations integrated in a GIS platform, *Cold Regions Science and Technology*, 54, 193–205, 2008.

Castebrunet, H., Eckert, N., and Giraud, G.: Snow and weather climatic control on snow avalanche occurrence fluctuations over 50 yr in the French Alps, *Climate of the Past*, 8, 855–875, <https://doi.org/10.5194/cp-8-855-2012>, 2012.

640 Castebrunet, H., Eckert, N., Giraud, G., Durand, Y., and Morin, S.: Projected changes of snow conditions and avalanche activity in a warming climate: the French Alps over the 2020-2050 and 2070-2100 periods, *The Cryosphere*, 8, 1673–1697, <https://doi.org/10.5194/tc-8-1673-2014>, 2014.

Chen, T. and Guestrin, C.: XGBoost: A Scalable Tree Boosting System, pp. 785–794, <https://doi.org/10.1145/2939672.2939785>, 2016.

Coles, S.: An Introduction to Statistical Modeling of Extreme Values, Springer London, London, ISBN 978-1-84996-874-4, <https://doi.org/10.1007/978-1-4471-3675-0>, 2001.



Corona, C., Lopez Saez, J., Stoffel, M., Bonnefoy, M., Richard, D., Astrade, L., and Berger, F.: How much of the real avalanche activity can be captured with tree rings? An evaluation of classic dendrogeomorphic approaches and comparison with historical archives, *Cold Regions Science and Technology*, 74-75, 31–42, [https://doi.org/https://doi.org/10.1016/j.coldregions.2012.01.003](https://doi.org/10.1016/j.coldregions.2012.01.003), 2012.

Decharme, B., Boone, A., Delire, C., and Noilhan, J.: Local evaluation of the Interaction between Soil Biosphere Atmosphere soil multilayer diffusion scheme using four pedotransfer functions, *Journal of Geophysical Research: Atmospheres*, 116, <https://doi.org/https://doi.org/10.1029/2011JD016002>, 2011.

Dumont, M., Monteiro, D., Filhol, S., Gascoin, S., Marty, C., Hagenmuller, P., Morin, S., Choler, P., and Thuiller, W.: The European Alps in a changing climate: physical trends and impacts, *Comptes Rendus. Géoscience*, 357, 25–42, <https://doi.org/10.5802/crgeos.288>, 2025.

Durand, Y., Giraud, G., Brun, E., Mérindol, L., and Martin, E.: A computer-based system simulating snowpack structures as a tool for regional avalanche forecasting, *Journal of Glaciology*, 45, 469–484, <https://doi.org/10.3189/S0022143000001337>, 1999.

Durand, Y., Giraud, G., Laternser, M., Etchevers, P., Mérindol, L., and Lesaffre, B.: Reanalysis of 47 Years of Climate in the French Alps (1958–2005): Climatology and Trends for Snow Cover, *Journal of Applied Meteorology and Climatology*, 48, 2487 – 2512, <https://doi.org/10.1175/2009JAMC1810.1>, 2009.

Eckert, N. and Giacoma, F.: Towards a holistic paradigm for long-term snow avalanche risk assessment and mitigation, *Ambio*, 52, 711–732, 2023.

Eckert, N., Baya, H., and Deschâtres, M.: Assessing the response of snow avalanche runout altitudes to climate fluctuations using hierarchical modeling: application to 61 winters of data in France, *Journal of Climate*, 23, 3157–3180, 2010a.

Eckert, N., Coleou, C., Castebrunet, H., Deschâtres, M., Giraud, G., and Gaume, J.: Cross-comparison of meteorological and avalanche data for characterising avalanche cycles: the example of December 2008 in the eastern part of the French Alps, *Cold Regions Science and Technology*, 64, 119–136, 2010b.

Eckert, N., Naaim, M., and Parent, E.: Long-term avalanche hazard assessment with a Bayesian depth-averaged propagation model, *Journal of Glaciology*, 56, 563–586, 2010c.

Eckert, N., Parent, E., Kies, R., and Baya, H.: A spatio-temporal modelling framework for assessing the fluctuations of avalanche occurrence resulting from climate change: application to 60 years of data in the northern French Alps, *Climatic change*, 101, 515–553, 2010d.

Eckert, N., Keylock, C., Bertrand, D., Parent, E., Faug, T., Favier, P., and Naaim, M.: Quantitative risk and optimal design approaches in the snow avalanche field: Review and extensions, *Cold Regions Science and Technology*, 79, 1–19, 2012.

Eckert, N., Keylock, C. J., Castebrunet, H., Lavigne, A., and Naaim, M.: Temporal trends in avalanche activity in the French Alps and subregions: from occurrences and runout altitudes to unsteady return periods, *Journal of Glaciology*, 59, 93–114, <https://doi.org/10.3189/2013JoG12J091>, 2013.

Eckert, N., Corona, C., and Giacoma, F.: Climate change impacts on snow avalanche activity and related risks, *Nature Reviews Earth and Environment*, 5, 369–389, <https://doi.org/10.1038/s43017-024-00540-2>, 2024.

European Avalanche Warning Services (EAWS): Typical Avalanche Problems, Approved by the General Assembly of EAWS, Davos, https://www.avalanches.org/wp-content/uploads/2022/09/EN_EAWS_avalanche_problems.pdf, 2022.

Evin, G., Dkengne Sielenou, P., Eckert, N., Naveau, P., Hagenmuller, P., and Morin, S.: Extreme avalanche cycles: Return levels and probability distributions depending on snow and meteorological conditions, *Weather and Climate Extremes*, 33, 100344, <https://doi.org/https://doi.org/10.1016/j.wace.2021.100344>, 2021.

Fischer, J.-T., Kofler, A., Huber, A., Fellin, W., Mergili, M., and Oberguggenberger, M.: Bayesian inference in snow avalanche simulation with r. avaflow, *Geosciences*, 10, 191, 2020.



Fuchs, S., Thöni, M., McAlpin, M. C., Gruber, U., and Bründl, M.: Avalanche hazard mitigation strategies assessed by cost effectiveness analyses and cost benefit analyses—evidence from Davos, Switzerland, *Natural Hazards*, 41, 113–129, 2007.

Fuchs, S., Keiler, M., Sokratov, S., and Shnyparkov, A.: Spatiotemporal dynamics: the need for an innovative approach in mountain hazard risk management, *Natural hazards*, 68, 1217–1241, 2013.

Fávero, L. P. L., Duarte, A., and Santos, H. P.: A New Computational Algorithm for Assessing Overdispersion and Zero-Inflation in Machine Learning Count Models with Python, *Computers*, 13, <https://www.mdpi.com/2073-431X/13/4/88>, 2024.

Giacona, F., Eckert, N., and Martin, B.: A 240-year history of avalanche risk in the Vosges Mountains based on non-conventional (re) sources, *Natural Hazards and Earth System Sciences*, 17, 887–904, 2017.

Giacona, F., Eckert, N., Corona, C., Mainieri, R., Morin, S., Stoffel, M., Martin, B., and Naaim, M.: Upslope migration of snow avalanches in a warming climate, *Proceedings of the National Academy of Sciences*, 118, e2107306 118, <https://doi.org/10.1073/pnas.2107306118>, 2021.

Giacona, F., Eckert, N., and Martin, B.: Comment interpréter une chronologie événementielle en géohistoire? L'exemple de deux siècles et demi d'avalanches dans le Massif vosgien, *Cybergeo: European Journal of Geography*, 2022.

Hafner, E. D., Techel, F., Leinss, S., and Bühler, Y.: Mapping avalanches with satellites – evaluation of performance and completeness, *The Cryosphere*, 15, 983–1004, <https://doi.org/10.5194/tc-15-983-2021>, 2021.

Heck, M., Hobiger, M., van Herwijnen, A., Schweizer, J., and Fäh, D.: Localization of seismic events produced by avalanches using multiple signal classification, *Geophysical Journal International*, 216, 201–217, <https://doi.org/10.1093/gji/ggy394>, 2018.

Hendrick, M., Techel, F., Volpi, M., Olevski, T., Pérez-Guillén, C., van Herwijnen, A., and Schweizer, J.: Automated prediction of wet-snow avalanche activity in the Swiss Alps, *Journal of Glaciology*, 69, 1–14, <https://doi.org/10.1017/jog.2023.24>, 2023.

Höller, P.: Avalanche hazards and mitigation in Austria: a review, *Natural Hazards*, 43, 81–101, <https://doi.org/10.1007/s11069-007-9109-2>, 2007.

Jacob, D., Petersen, J., Eggert, B., Alias, A., Christensen, O. B., Bouwer, L. M., Braun, A., Colette, A., Déqué, M., Georgievski, G., Georgopoulou, E., Gobiet, A., Menut, L., Nikulin, G., Haensler, A., Hempelmann, N., Jones, C., Keuler, K., Kovats, S., Kröner, N., Kotlarski, S., Kriegsmann, A., Martin, E., van Meijgaard, E., Moseley, C., Pfeifer, S., Preuschmann, S., Radermacher, C., Radtke, K., Rechid, D., Rounsevell, M., Samuelsson, P., Somot, S., Soussana, J.-F., Teichmann, C., Valentini, R., Vautard, R., Weber, B., and Yiou, P.: EURO-CORDEX: new high-resolution climate change projections for European impact research, *Regional Environmental Change*, 14, 563–578, <https://doi.org/10.1007/s10113-013-0499-2>, 2014.

Jakob Themeßl, M., Gobiet, A., and Leuprecht, A.: Empirical-statistical downscaling and error correction of daily precipitation from regional climate models, *International Journal of Climatology*, 31, 1530–1544, <https://doi.org/10.1002/joc.2168>, 2011.

Johnson, A. L. and Smith, D. J.: Geomorphology of snow avalanche impact landforms in the southern Canadian Cordillera, *Canadian Geographies / Géographies canadiennes*, 54, 87–103, <https://doi.org/10.1111/j.1541-0064.2009.00275.x>, 2010.

Karas, A., Karbou, F., Giffard-Roisin, S., Durand, P., and Eckert, N.: Automatic Color Detection-Based Method Applied to Sentinel-1 SAR Images for Snow Avalanche Debris Monitoring, *IEEE Transactions on Geoscience and Remote Sensing*, 60, 1–17, <https://doi.org/10.1109/TGRS.2021.3131853>, 2022.

Kern, H., Jomelli, V., Eckert, N., Grancher, D., and Deschâtres, M.: Variability of avalanche deposits volumes and relationships with corridor morphology (Bessans, Savoie, France), 2020.

Kotlarski, S., AU, Gobiet, A., Morin, S., Olefs, M., Rajczak, J., and Samacoïts, R.: 21st Century alpine climate change, *Climate Dynamics*, 60, 65–86, <https://doi.org/10.1007/s00382-022-06303-3>, 2023.



Kronholm, K., Vikhamar-Schuler, D., Jaedicke, C., Isaksen, K., Sorteberg, A., and Kristensen, K.: Forecasting snow avalanche days from meteorological data using classification trees; Grasdalen, western Norway, 2006.

Lazar, B. and Williams, M.: Climate change in western ski areas: Potential changes in the timing of wet avalanches and snow quality for the Aspen ski area in the years 2030 and 2100, *Cold Regions Science and Technology*, 51, 219–228, 725 <https://doi.org/https://doi.org/10.1016/j.coldregions.2007.03.015>, international Snow Science Workshop (ISSW) 2006, 2008.

Le Roux, E., Evin, G., Eckert, N., Blanchet, J., and Morin, S.: A non-stationary extreme-value approach for climate projection ensembles: application to snow loads in the French Alps, *Earth System Dynamics*, 13, 1059–1075, <https://doi.org/10.5194/esd-13-1059-2022>, 2022.

Le Roux, E., Evin, G., Samacoïts, R., Eckert, N., Blanchet, J., and Morin, S.: Projection of snowfall extremes in the French Alps as a function 730 of elevation and global warming level, *The Cryosphere*, 17, 4691–4704, <https://doi.org/10.5194/tc-17-4691-2023>, 2023.

Mainieri, R., Favillier, A., Lopez-Saez, J., Eckert, N., Zgheib, T., Morel, P., Saulnier, M., Peiry, J.-L., Stoffel, M., and Corona, C.: Impacts of land-cover changes on snow avalanche activity in the French Alps, *Anthropocene*, 30, 100 244, 2020.

Marty, C., Schlägl, S., Bavay, M., and Lehning, M.: How much can we save? Impact of different emission scenarios on future snow cover in the Alps, *The Cryosphere*, 11, 517–529, <https://doi.org/10.5194/tc-11-517-2017>, 2017.

735 Masson, D. and Frei, C.: Long-term variations and trends of mesoscale precipitation in the Alps: Recalculation and update for 1901–2008, *International Journal of Climatology*, 36, <https://doi.org/10.1002/joc.4343>, 2015.

Matiu, M., Crespi, A., Bertoldi, G., Carmagnola, C. M., Marty, C., Morin, S., Schöner, W., Cat Berro, D., Chiogna, G., De Gregorio, L., Kotlarski, S., Majone, B., Resch, G., Terzago, S., Valt, M., Beozzo, W., Cianfarra, P., Gouttevin, I., Marcolini, G., Notarnicola, C., Petitta, M., Scherrer, S. C., Strasser, U., Winkler, M., Zebisch, M., Cicogna, A., Cremonini, R., Debernardi, A., Faletto, M., Gaddo, M., 740 Giovannini, L., Mercalli, L., Soubeyroux, J.-M., Sušnik, A., Trenti, A., Urbani, S., and Weilguni, V.: Observed snow depth trends in the European Alps: 1971 to 2019, *The Cryosphere*, 15, 1343–1382, <https://doi.org/10.5194/tc-15-1343-2021>, 2021.

Matiu, M., Napoli, A., Kotlarski, S., Zardi, D., Bellin, A., and Majone, B.: Elevation-dependent biases of raw and bias-adjusted EURO-745 CORDEX regional climate models in the European Alps, *Climate Dynamics*, 62, 9013–9030, <https://doi.org/10.1007/s00382-024-07376-y>, 2024.

Maurer, E. P. and Pierce, D. W.: Bias correction can modify climate model simulated precipitation changes without adverse effect on the ensemble mean, *Hydrology and Earth System Sciences*, 18, 915–925, <https://doi.org/10.5194/hess-18-915-2014>, 2014.

Mayer, S., van Herwijnen, A., Techel, F., and Schweizer, J.: A random forest model to assess snow instability from simulated snow stratigraphy, *The Cryosphere*, 16, 4593–4615, <https://doi.org/10.5194/tc-16-4593-2022>, 2022.

Mayer, S., Hendrick, M., Michel, A., Richter, B., Schweizer, J., Wernli, H., and van Herwijnen, A.: Changes in snow avalanche activity in 750 response to climate warming in the Swiss Alps, *EGUsphere*, 2024, 1–32, <https://doi.org/10.5194/egusphere-2024-1026>, 2024.

McClung, D. M.: Fracture mechanical models of dry slab avalanche release, *Journal of Geophysical Research: Solid Earth*, 86, 10 783–10 790, <https://doi.org/https://doi.org/10.1029/JB086iB11p10783>, 1981.

Mitterer, C. and Schweizer, J.: Analysis of the snow-atmosphere energy balance during wet-snow instabilities and implications for avalanche prediction, *The Cryosphere*, 7, 205–216, <https://doi.org/10.5194/tc-7-205-2013>, 2013.

755 Moen, J., Aune, K., Edenius, L., and Angerbjörn, A.: Potential Effects of Climate Change on Treeline Position in the Swedish Mountains, *Ecology and Society*, 9, <http://www.jstor.org/stable/26267652>, 2004.

Mott, R., Schirmer, M., Bavay, M., Grünwald, T., and Lehning, M.: Understanding snow-transport processes shaping the mountain snow-cover, *The Cryosphere*, 4, 545–559, <https://doi.org/10.5194/tc-4-545-2010>, 2010.



Nakicenović, N. and Swart, R., eds.: Special Report on Emissions Scenarios: A Special Report of Working Group III of the Intergovernmental
760 Panel on Climate Change, Cambridge University Press, Cambridge, UK, ISBN 0-521-80493-0, <http://digitallibrary.un.org/record/466938>,
2000.

Orhobor, O. I., Grinberg, N. F., Soldatova, L. N., and King, R. D.: Imbalanced regression using regressor-classifier ensembles, *Machine
Learning*, 112, 1365–1387, <https://doi.org/10.1007/s10994-022-06199-4>, 2023.

Ortner, G., A., M., and Kropf, C.: Assessing the impacts of climate change on snow avalanche-induced risk in alpine regions, *Nat Hazards*,
765 <https://doi.org/https://doi.org/10.1007/s11069-025-07229-9>, 2025.

Peitzsch, E. H., Pederson, G. T., Birkeland, K. W., Hendrikx, J., and Fagre, D. B.: Climate drivers of large magnitude snow avalanche years
in the U.S. northern Rocky Mountains, *Scientific Reports*, 11, 10 032, <https://doi.org/10.1038/s41598-021-89547-z>, 2021.

Reuter, B., Viallon-Galinier, L., Horton, S., Herwijnen, A., Mayer, S., Hagenmuller, P., and Morin, S.: Characterizing snow instability
770 with avalanche problem types derived from snow cover simulations, *Cold Regions Science and Technology*, 194, 103 462,
<https://doi.org/https://doi.org/10.1016/j.coldregions.2021.103462>, 2022.

Reuter, B., Hagenmuller, P., and Eckert, N.: Trends in avalanche problems in the French Alps between 1958 and 2020, *Cold Regions Science
and Technology*, 238, 104 555, <https://doi.org/https://doi.org/10.1016/j.coldregions.2025.104555>, 2025.

Roch: Les déclenchements d'avalanche, *Symposium at Davos*, p. 86–99, 1966.

Rožanec, J. M., Petelin, G., Costa, J., Bertalanič, B., Cerar, G., Guček, M., Papa, G., and Mladenić, D.: Dealing with zero-inflated data:
775 achieving SOTA with a two-fold machine learning approach, <https://arxiv.org/abs/2310.08088>, 2023.

Schneebeli, M. and Sokratov, S.: Tomography of temperature gradient metamorphism of snow and associated changes in heat conductivity,
Hydrological Processes, 18, 3655 – 3665, <https://doi.org/10.1002/hyp.5800>, 2004.

Schweizer, J., Jamieson, B., and Schneebeli, M.: Snow avalanche formation, *Reviews of Geophysics*, 41, 1016,
<https://doi.org/10.1029/2002RG000123>, 2003.

Serquet, G., Marty, C., Duxley, J.-P., and Rebetez, M.: Seasonal trends and temperature dependence of the snowfall/precipitation-day ratio in
780 Switzerland, *Geophysical Research Letters*, 38, <https://doi.org/https://doi.org/10.1029/2011GL046976>, 2011.

Sielenou, P. D., Viallon-Galinier, L., Hagenmuller, P., Naveau, P., Morin, S., Dumont, M., Verfaillie, D., and Eckert, N.: Combining random
forests and class-balancing to discriminate between three classes of avalanche activity in the French Alps, *Cold Regions Science and
Technology*, 187, 103 276, <https://doi.org/https://doi.org/10.1016/j.coldregions.2021.103276>, 2021.

Smiatek, G., Kunstmann, H., and Senator, A.: EURO-CORDEX regional climate model analysis for the Greater Alpine
Region: Performance and expected future change, *Journal of Geophysical Research: Atmospheres*, 121, 7710–7728,
<https://doi.org/https://doi.org/10.1002/2015JD024727>, 2016.

Techel, F., Jarry, F., Kronthaler, G., Mitterer, S., Nairz, P., Pavsek, M., Valt, M., and Darms, G.: Avalanche fatalities in the European Alps:
Long-term trends and statistics, *Geographica Helvetica*, 71, 147–159, <https://doi.org/10.5194/gh-71-147-2016>, 2016.

Teich, M., Zurbiggen, N., Bartelt, P., Grêt-Regamey, A., Marty, C., Ulrich, M., and Bebi, P.: POTENTIAL IMPACTS OF CLIMATE
790 CHANGE ON SNOW AVALANCHES STARTING IN FORESTED TERRAIN, 2012.

Uppala, S. M., Källberg, P. W., Simmons, A. J., Andrae, U., Bechtold, V. D. C., Fiorino, M., Gibson, J. K., Haseler, J., Hernandez, A., Kelly,
G. A., Li, X., Onogi, K., Saarinen, S., Sokka, N., Allan, R. P., Andersson, E., Arpe, K., Balmaseda, M. A., Beljaars, A. C. M., Berg, L.
V. D., Bidlot, J., Bormann, N., Caires, S., Chevallier, F., Dethof, A., Dragosavac, M., Fisher, M., Fuentes, M., Hagemann, S., Hólm, E.,
795 Hoskins, B. J., Isaksen, L., Janssen, P. A. E. M., Jenne, R., McNally, A. P., Mahfouf, J.-F., Morcrette, J.-J., Rayner, N. A., Saunders, R. W.,



Simon, P., Sterl, A., Trenberth, K. E., Untch, A., Vasiljevic, D., Viterbo, P., and Woollen, J.: The ERA-40 re-analysis, *Quarterly Journal of the Royal Meteorological Society*, 131, 2961–3012, [https://doi.org/https://doi.org/10.1256/qj.04.176](https://doi.org/10.1256/qj.04.176), 2005.

Van Vuuren, D., Edmonds, J. A., Kainuma, M., Riahi, K., Thomson, A. M., Hibbard, K. A., Hurtt, G., Kram, T., Krey, V., Lamarque, J.-F., et al.: The Representative Concentration Pathways: An Overview, *Climatic Change*, 109, <https://www.osti.gov/biblio/1029075>, 2011.

800 Vautard, R., Kadygrov, N., Iles, C., Boberg, F., Buonomo, E., Bülow, K., Coppola, E., Corre, L., van Meijgaard, E., Nogherotto, R., Sandstad, M., Schwingshackl, C., Somot, S., Aalbers, E., Christensen, O. B., Ciarlo, J. M., Demory, M.-E., Giorgi, F., Jacob, D., Jones, R. G., Keuler, K., Kjellström, E., Lenderink, G., Levavasseur, G., Nikulin, G., Sillmann, J., Solidoro, C., Sørland, S. L., Steger, C., Teichmann, C., Warrach-Sagi, K., and Wulfmeyer, V.: Evaluation of the Large EURO-CORDEX Regional Climate Model Ensemble, *Journal of Geophysical Research: Atmospheres*, 126, e2019JD032344, <https://doi.org/https://doi.org/10.1029/2019JD032344>, e2019JD032344 2019JD032344, 2021.

Verfaillie, D., Déqué, M., Morin, S., and Lafaysse, M.: The method ADAMONT v1.0 for statistical adjustment of climate projections applicable to energy balance land surface models, *Geoscientific Model Development*, 10, 4257–4283, <https://doi.org/10.5194/gmd-10-4257-2017>, 2017.

810 Verfaillie, D., Lafaysse, M., Déqué, M., Eckert, N., Lejeune, Y., and Morin, S.: Multi-component ensembles of future meteorological and natural snow conditions for 1500m altitude in the Chartreuse mountain range, Northern French Alps, *The Cryosphere*, 12, 1249–1271, <https://doi.org/10.5194/tc-12-1249-2018>, 2018.

Vernay, M., Lafaysse, M., Monteiro, D., Hagenmuller, P., Nheili, R., Samacoits, R., Verfaillie, D., and Morin, S.: The S2M meteorological and snow cover reanalysis over the French mountainous areas: description and evaluation (1958–2021), *Earth System Science Data*, 14, 1707–1733, <https://doi.org/10.5194/essd-14-1707-2022>, 2022.

815 Viallon-Galinier, L., Hagenmuller, P., and Eckert, N.: Combining modelled snowpack stability with machine learning to predict avalanche activity, *The Cryosphere*, 17, 2245–2260, <https://doi.org/10.5194/tc-17-2245-2023>, 2023.

Vionnet, V., Brun, E., Morin, S., Boone, A., Faroux, S., Le Moigne, P., Martin, E., and Willemet, J.-M.: The detailed snowpack scheme Crocus and its implementation in SURFEX v7.2, *Geoscientific Model Development*, 5, 773–791, <https://doi.org/10.5194/gmd-5-773-2012>, 2012.

Wang, Z., Goetz, J., and Brenning, A.: Transfer learning for landslide susceptibility modeling using domain adaptation and case-based reasoning, *Geoscientific Model Development*, 15, 8765–8784, <https://doi.org/10.5194/gmd-15-8765-2022>, 2022.

820 Ying, X.: An Overview of Overfitting and its Solutions, *Journal of Physics: Conference Series*, 1168, 022 022, <https://doi.org/10.1088/1742-6596/1168/2/022022>, 2019.

Young, D. S., Roemmele, E. S., and Yeh, P.: Zero-inflated modeling part I: Traditional zero-inflated count regression models, their applications, and computational tools, *WIREs Computational Statistics*, 14, e1541, <https://doi.org/https://doi.org/10.1002/wics.1541>, 2022.

825 Zgheib, T., Giacoma, F., Granet-Abisset, A.-M., Morin, S., and Eckert, N.: One and a half century of avalanche risk to settlements in the upper Maurienne valley inferred from land cover and socio-environmental changes., *Global Environmental Change*, 65, 102 149, <https://doi.org/https://doi.org/10.1016/j.gloenvcha.2020.102149>, 2020.

Zgheib, T., Giacoma, F., Granet-Abisset, A.-M., Morin, S., Lavigne, A., and Eckert, N.: Spatio-temporal variability of avalanche risk in the French Alps, *Regional Environmental Change*, 22, 8, 2022.